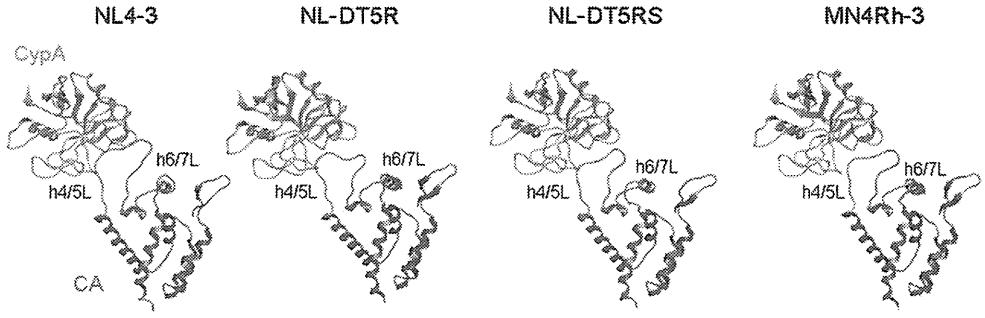

	NL4-3	NL-DT5R	NL-DT5RS	MN4Rh-3
CA	HIV-1 CA	h4/5L from SIVmac239	h4/5L and h6/7L from SIVmac239	h4/5L and h6/7L from SIVmac239 and Q110D
Binding energy (kcal/mol)	-64.447	-31.012	-36.071	-30.051

Fig. 6. Structural models of HIV CA NTD bound to CypA. The model of CA NTD bound to CypA was constructed by homology modeling using the crystal structure of HIV-1 CA NTD and CypA complex (PDB code: 1M9C [28]). The binding energies, E_{bind} (kcal/mol), of the complex were calculated using MOE as described previously [42,43]. The formula $E_{bind} = E_{complex} - (E_{CA} + E_{CypA})$ was used for the E_{bind} calculation, where $E_{complex}$ is the energy of the CA/CypA complex models, E_{CA} is the energy of the CA monomer model, and E_{CypA} is the energy of the CypA monomer model.

domain [46]. Thus, it is not unreasonable to assume that the replication of MN4Rh-3 carrying CA-Q110D is enhanced in macaque cells but reduced in human cells by augmenting its dissociation from CypA (Fig. 6). However, it was found to be difficult to experimentally confirm this structural insight by determining the effect of cyclosporine A or of siRNA against CypA on viral infectivity because interaction between the HIV-1mt CA and CypA was so weak. Alternatively, CA-Q110D may contribute to the alteration of the affinity to unknown anti-CA factor(s) other than CypA and TRIM5 proteins. In this case, it is speculated that the factor(s) might act negatively on HIV-1 replication in macaque cells but positively in human cells, and vice versa. Further study is required to elucidate the mechanism for enhancement of viral growth potential by CA-Q110D.

In conclusion, further modification of the HIV-1mt genome is necessary to overcome unconquered replication block(s) present in macaque cells and obtain viral clones similarly replication-competent in macaque cells and pathogenic for animals with SIVmac (Fig. 5). Considering the genome structure of MN4Rh-3 and the results presented here, major targets for modification now are *gag*-CA (against TRIM5α) and *vpu* (against tetherin). Gag-CA is one of the two principal viral determinants (CA and Vif) for the HIV-1 species-tropism. Construction of HIV-1 CA that evades from TRIM5α restriction is also useful for elucidation of the less-defined CA-TRIM5α interaction and antiviral mechanism of TRIM5α. Tetherin, identified as anti-virion release factor, is antagonized by Vpu [47,48], but macaque tetherin was not counteracted by HIV-1 Vpu [49]. Construction of HIV-1 Vpu that down-modulate macaque tetherin may enhance viral replication *in vivo* as well as *in vitro* [50]. Through these approaches, we may be able to precisely analyze HIV-1 replication and pathogenesis *in vivo* and provide new strategies against HIV-1/AIDS.

Acknowledgments

This study was supported by a grant from the Ministry of Health, Labor and Welfare of Japan (Research on HIV/AIDS project no. H23-003).

References

[1] M.H. Malim, M. Emerman, HIV-1 accessory proteins–ensuring viral survival in a hostile environment, Cell Host Microbe 3 (2008) 388–398.
[2] F. Kirchhoff, Immune evasion and counteraction of restriction factors by HIV-1 and other primate lentiviruses, Cell Host Microbe 8 (2010) 55–67.
[3] R. Shibata, H. Sakai, M. Kawamura, K. Tokunaga, A. Adachi, Early replication block of human immunodeficiency virus type 1 in monkey cells, J. Gen. Virol. 76 (1995) 2723–2730.
[4] M. Nomaguchi, N. Doi, K. Kamada, A. Adachi, Species barrier of HIV-1 and its jumping by virus engineering, Rev. Med. Virol. 18 (2008) 261–275.
[5] M. Nomaguchi, A. Adachi, Virology as biosystematics: towards understanding the viral infection biology, Front. Microbiol. 1 (2010) 2.
[6] R.K. Holmes, M.H. Malim, K.N. Bishop, APOBEC-mediated viral restriction: not simply editing? Trends Biochem. Sci. 32 (2007) 118–128.
[7] H. Huthoff, G.J. Towers, Restriction of retroviral replication by APOBEC3G/F and TRIM5alpha, Trends Microbiol. 16 (2008) 612–619.
[8] K. Strebel, J. Luban, K.T. Jeang, Human cellular restriction factors that target HIV-1 replication, BMC Med. 7 (2009) 48.
[9] J. Luban, Cyclophilin A, TRIM5, and resistance to human immunodeficiency virus type 1 infection, J. Virol. 81 (2007) 1054–1061.
[10] G.J. Towers, The control of viral infection by tripartite motif proteins and cyclophilin A, Retrovirology 4 (2007) 40.
[11] E.E. Nakayama, T. Shioda, Anti-retroviral activity of TRIM5 alpha, Rev. Med. Virol. 20 (2010) 77–92.
[12] R.M. Newman, L. Hall, M. Connole, G.L. Chen, S. Sato, E. Yuste, W. Diehl, E. Hunter, A. Kaur, G.M. Miller, W.E. Johnson, Balancing selection and the evolution of functional polymorphism in old world monkey TRIM5alpha, Proc. Natl. Acad. Sci. U. S. A. 103 (2006) 19134–19139.
[13] S.J. Wilson, B.L. Webb, L.M. Ylinen, E. Verschoor, J.L. Heeney, G.J. Towers, Independent evolution of an antiviral TRIMCyp in rhesus macaques, Proc. Natl. Acad. Sci. U. S. A. 105 (2008) 3557–3562.

[14] A.J. Price, F. Marzetta, M. Lammers, L.M. Ylinen, T. Schaller, S.J. Wilson, G.J. Towers, L.C. James, Active site remodeling switches HIV specificity of antiretroviral TRIMCyp, Nat. Struct. Mol. Biol. 16 (2009) 1036–1042.
[15] L.M. Ylinen, A.J. Price, J. Rasaiyaah, S. Hué, N.J. Rose, F. Marzetta, L.C. James, G.J. Towers, Conformational adaptation of Asian macaque TRIMCyp directs lineage specific antiviral activity, PLoS Pathog. 6 (2010) e1001062.
[16] K. Kamada, T. Igarashi, M.A. Martin, B. Khamsri, K. Hatcho, T. Yamashita, M. Fujita, T. Uchiyama, A. Adachi, Generation of HIV-1 derivatives that productively infect macaque monkey lymphoid cells, Proc. Natl. Acad. Sci. U. S. A. 103 (2006) 16959–16964.
[17] T. Igarashi, R. Iyengar, R.A. Byrum, A. Buckler-White, R.L. Dewar, C.E. Buckler, H.C. Lane, K. Kamada, A. Adachi, M.A. Martin, Human immunodeficiency virus type 1 derivative with 7% simian immunodeficiency virus genetic content is able to establish infections in pig-tailed macaques, J. Virol. 81 (2007) 11549–11552.
[18] K. Kamada, T. Yamashita, K. Hatcho, A. Adachi, M. Nomaguchi, Evasion from CypA- and APOBEC-mediated restrictions is insufficient for HIV-1 to efficiently grow in simian cells, Microbes Infect. 11 (2009) 164–171.
[19] A. Saito, M. Nomaguchi, S. Iijima, A. Kuroishi, T. Yoshida, Y.J. Lee, T. Hayakawa, K. Kono, E.E. Nakayama, T. Shioda, Y. Yasutomi, A. Adachi, T. Matano, H. Akari, Improved capacity of a monkey-tropic HIV-1 derivative to replicate in cynomolgus monkeys with minimal modifications, Microbes Infect. 13 (2011) 58–64.
[20] A. Kuroishi, A. Saito, Y. Shingai, T. Shioda, M. Nomaguchi, A. Adachi, H. Akari, E.E. Nakayama, Modification of a loop sequence between alpha-helices 6 and 7 of virus capsid (CA) protein in a human immunodeficiency virus type 1 (HIV-1) derivative that has simian immunodeficiency virus (SIVmac239) vif and CA alpha-helices 4 and 5 loop improves replication in cynomolgus monkey cells, Retrovirology 6 (2009) 70.
[21] T. Yamashita, N. Doi, A. Adachi, M. Nomaguchi, Growth ability in simian cells of monkey cell-tropic HIV-1 is greatly affected by downstream region of the vif gene, J. Med. Invest. 55 (2008) 236–240.
[22] M. Yamashita, M. Emerman, Capsid is a dominant determinant of retrovirus infectivity in nondividing cells, J. Virol. 78 (2004) 5670–5678.
[23] J.S. Lebkowski, S. Clancy, M.P. Calos, Simian virus 40 replication in adenovirus-transformed human cells antagonizes gene expression, Nature 317 (1985) 169–171.
[24] H. Akari, T. Fukumori, S. Iida, A. Adachi, Induction of apoptosis in herpesvirus saimiri-immortalized T lymphocytes by blocking interaction of CD28 with CD80/CD86, Biochem. Biophys. Res. Commun. 263 (1999) 352–356.
[25] N. Doi, S. Fujiwara, A. Adachi, M. Nomaguchi, Growth ability in various macaque cell lines of HIV-1 with simian cell-tropism, J. Med. Invest. 57 (2010) 284–292.
[26] A. Adachi, H.E. Gendelman, S. Koenig, T. Folks, R. Willey, A. Rabson, M.A. Martin, Production of acquired immunodeficiency syndrome-associated retrovirus in human and nonhuman cells transfected with an infectious molecular clone, J. Virol. 59 (1986) 284–291.
[27] U. O'Doherty, W.J. Swiggard, M.H. Malim, Human immunodeficiency virus type 1 spinoculation enhances infection through virus binding, J. Virol. 74 (2004) 10074–10080.
[28] B.R. Howard, F.F. Vajdos, S. Li, W.I. Sundquist, C.P. Hill, Structural insights into the catalytic mechanism of cyclophilin A, Nat. Struct. Biol. 10 (2003) 475–481.
[29] N. Deshpande, K.J. Addess, W.F. Bluhm, J.C. Merino-Ott, W. Townsend-Merino, Q. Zhang, C. Knezevich, L. Xie, L. Chen, Z. Feng, R.K. Green, J.L. Flippen-Anderson, J. Westbrook, H.M. Berman, P.E. Bourne, The RCSB protein data bank: a redesigned query system and relational database based on the mmCIF schema, Nucleic Acids Res. 33 (Database issue) (2005) D233–D237.
[30] H. Song, E.E. Nakayama, M. Yokoyama, H. Sato, J.A. Levy, T. Shioda, A single amino acid of the human immunodeficiency virus type 2 capsid affects its replication in the presence of cynomolgus monkey and human TRIM5alphas, J. Virol. 81 (2007) 7280–7285.
[31] K. Kono, H. Song, M. Yokoyama, H. Sato, T. Shioda, E.E. Nakayama, Multiple sites in the N-terminal half of simian immunodeficiency virus capsid protein contribute to evasion from rhesus monkey TRIM5α-mediated restriction, Retrovirology 7 (2010) 72.
[32] N. Inagaki, H. Takeuchi, M. Yokoyama, H. Sato, A. Ryo, H. Yamamoto, M. Kawada, T. Matano, A structural constraint for functional interaction between N-terminal and C-terminal domains in simian immunodeficiency virus capsid proteins, Retrovirology 7 (2010) 90.
[33] P. Labute, The generalized Born/volume integral implicit solvent model: estimation of the free energy of hydration using London dispersion instead of atomic surface area, J. Comput. Chem. 29 (2008) 1693–1698.
[34] J.W. Ponder, D.A. Case, Force fields for protein simulations, Adv. Protein Chem. 66 (2003) 27–85.
[35] A. Onufriev, D. Bashford, D.A. Case, Modification of the generalized Born model suitable for macromolecules, J. Phys. Chem. B 104 (2000) 3712–3720.
[36] T.Y. Lin, M. Emerman, Determinants of cyclophilin A-dependent TRIM5 alpha restriction against HIV-1, Virology 379 (2008) 335–341.
[37] A. Kuroishi, K. Bozek, T. Shioda, E.E. Nakayama, A single amino acid substitution of the human immunodeficiency virus type 1 capsid protein affects viral sensitivity to TRIM5 alpha, Retrovirology 7 (2010) 58.
[38] M. Stremlau, C.M. Owens, M.J. Perron, M. Kiessling, P. Autissier, J. Sodroski, The cytoplasmic body component TRIM5alpha restricts HIV-1 infection in old world monkeys, Nature 427 (2004) 848–853.
[39] Z. Keckesova, L.M. Ylinen, G.J. Towers, Cyclophilin A renders human immunodeficiency virus type 1 sensitive to old world monkey but not human TRIM5 alpha antiviral activity, J. Virol. 80 (2006) 4683–4690.
[40] E. Sokolskaja, L. Berthoux, J. Luban, Cyclophilin A and TRIM5alpha independently regulate human immunodeficiency virus type 1 infectivity in human cells, J. Virol. 80 (2006) 2855–2862.
[41] S.Y. Lim, T. Rogers, T. Chan, J.B. Whitney, J. Kim, J. Sodroski, N.L. Letvin, TRIM5alpha modulates immunodeficiency virus control in rhesus monkeys, PLoS Pathog. 6 (2010) e1000738.
[42] C.O. Onyango, A. Leligdowicz, M. Yokoyama, H. Sato, H. Song, E.E. Nakayama, T. Shioda, T. de Silva, J. Townend, A. Jaye, H. Whittle, S. Rowland-Jones, M. Cotten, HIV-2 capsids distinguish high and low virus load patients in a West African community cohort, Vaccine 28 (2010) B60–B67.
[43] M. Kinomoto, R. Appiah-Opong, J.A. Brandful, M. Yokoyama, N. Nii-Trebi, E. Ugly-Kwame, H. Sato, D. Ofori-Adjei, T. Kurata, F. Barre-Sinoussi, T. Sata, K. Tokunaga, HIV-1 proteases from drug-naive West African patients are differentially less susceptible to protease inhibitors, Clin. Infect. Dis. 41 (2005) 243–251.
[44] R.K. Gitti, B.M. Lee, J. Walker, M.F. Summers, S. Yoo, W.I. Sundquist, Structure of the amino-terminal core domain of the HIV-1 capsid protein, Science 273 (1996) 231–235.
[45] C. Tang, Y. Ndassa, M.F. Summers, Structure of the N-terminal 283-residue fragment of the immature HIV-1 Gag polyprotein, Nat. Struct. Biol. 9 (2002) 537–543.
[46] M. Yokoyama, S. Naganawa, K. Yoshimura, S. Matsushita, H. Sato, Structural dynamics of HIV-1 envelope Gp120 outer domain with V3 loop, PLoS One 7 (2012) e37530.
[47] S.J. Neil, T. Zang, P.D. Bieniasz, Tetherin inhibits retrovirus release and is antagonized by HIV-1 Vpu, Nature 451 (2008) 425–430.
[48] N. Van Damme, D. Goff, C. Katsura, R.L. Jorgenson, R. Mitchell, M.C. Johnson, E.B. Stephens, J. Guatelli, The interferon-induced protein BST-2 restricts HIV-1 release and is downregulated from the cell surface by the viral Vpu protein, Cell Host Microbe 3 (2008) 245–252.
[49] D. Sauter, M. Schindler, A. Specht, W.N. Landford, J. Münch, K.A. Kim, J. Votteler, U. Schubert, F. Bibollet-Ruche, B.F. Keele, J. Takehisa, Y. Ogando, C. Ochsenbauer, J.C. Kappes, A. Ayouba, M. Peeters, G.H. Learn, G. Shaw, P.M. Sharp, P. Bieniasz, B.H. Hahn, T. Hatziioannou, F. Kirchhoff, Tetherin-driven adaptation of Vpu and Nef function and the evolution of pandemic and nonpandemic HIV-1 strains, Cell Host Microbe 6 (2009) 409–421.
[50] M. Shingai, T. Yoshida, M.A. Martin, K. Strebel, Some human immunodeficiency virus type 1 Vpu proteins are able to antagonize macaque BST-2 in vitro and in vivo: Vpu-negative simian-human immunodeficiency viruses are attenuated in vivo, J. Virol. 85 (2011) 9708–9715.

PLOS ONE

A Novel Protective MHC-I Haplotype Not Associated with Dominant Gag-Specific CD8$^+$ T-Cell Responses in SIVmac239 Infection of Burmese Rhesus Macaques

Naofumi Takahashi[1,2], Takushi Nomura[1,2], Yusuke Takahara[1,2], Hiroyuki Yamamoto[1], Teiichiro Shiino[1], Akiko Takeda[1], Makoto Inoue[3], Akihiro Iida[3], Hiroto Hara[3], Tsugumine Shu[3], Mamoru Hasegawa[3], Hiromi Sakawaki[4], Tomoyuki Miura[4], Tatsuhiko Igarashi[4], Yoshio Koyanagi[4], Taeko K. Naruse[5], Akinori Kimura[5], Tetsuro Matano[1,2]*

1 AIDS Research Center, National Institute of Infectious Diseases, Tokyo, Japan, **2** The Institute of Medical Science, The University of Tokyo, Tokyo, Japan, **3** DNAVEC Corporation, Tsukuba, Japan, **4** Institute for Virus Research, Kyoto University, Kyoto, Japan, **5** Department of Molecular Pathogenesis, Medical Research Institute, Tokyo Medical and Dental University, Tokyo, Japan

Abstract

Several major histocompatibility complex class I (MHC-I) alleles are associated with lower viral loads and slower disease progression in human immunodeficiency virus (HIV) and simian immunodeficiency virus (SIV) infections. Immune-correlates analyses in these MHC-I-related HIV/SIV controllers would lead to elucidation of the mechanism for viral control. Viral control associated with some protective MHC-I alleles is attributed to CD8$^+$ T-cell responses targeting Gag epitopes. We have been trying to know the mechanism of SIV control in multiple groups of Burmese rhesus macaques sharing MHC-I genotypes at the haplotype level. Here, we found a protective MHC-I haplotype, *90-010-Id* (D), which is not associated with dominant Gag-specific CD8$^+$ T-cell responses. Viral loads in five D$^+$ animals became significantly lower than those in our previous cohorts after 6 months. Most D$^+$ animals showed predominant Nef-specific but not Gag-specific CD8$^+$ T-cell responses after SIV challenge. Further analyses suggested two Nef-epitope-specific CD8$^+$ T-cell responses exerting strong suppressive pressure on SIV replication. Another set of five D$^+$ animals that received a prophylactic vaccine using a Gag-expressing Sendai virus vector showed significantly reduced viral loads compared to unvaccinated D$^+$ animals at 3 months, suggesting rapid SIV control by Gag-specific CD8$^+$ T-cell responses in addition to Nef-specific ones. These results present a pattern of SIV control with involvement of non-Gag antigen-specific CD8$^+$ T-cell responses.

Citation: Takahashi N, Nomura T, Takahara Y, Yamamoto H, Shiino T, et al. (2013) A Novel Protective MHC-I Haplotype Not Associated with Dominant Gag-Specific CD8$^+$ T-Cell Responses in SIVmac239 Infection of Burmese Rhesus Macaques. PLoS ONE 8(1): e54300. doi:10.1371/journal.pone.0054300

Editor: Douglas F. Nixon, University of California San Francisco, United States of America

Received November 13, 2012; **Accepted** December 10, 2012; **Published** January 14, 2013

Funding: This work was supported by grants-in-aid from the Ministry of Education, Culture, Sports, Science, and Technology, and grants-in-aid from the Ministry of Health, Labor, and Welfare. The funders had no role in study design, data collection and analysis, decision to publish, or preparation of the manuscript.

Competing Interests: Makoto Inoue, Akihiro Iida, Hiroto Hara, Tsugumine Shu and Mamoru Hasegawa are employed by DNAVEC Corporation. There are no patents, products in development or marketed products to declare. This does not alter the authors' adherence to all the PLOS ONE policies on sharing data and materials, as detailed online in the guide for authors.

* E-mail: tmatano@nih.go.jp

Introduction

Virus-specific CD8$^+$ T-cell responses play a central role in the control of human immunodeficiency virus (HIV) and simian immunodeficiency virus (SIV) replication [1,2,3,4,5]. Genetic diversities of HLA or major histocompatibility complex class I (MHC-I) result in various patterns of CD8$^+$ T-cell responses in HIV-infected individuals. Cumulative studies on HIV infection have indicated the association of MHC-I genotypes with higher or lower viral loads [6,7,8,9,10]. In some MHC-1 alleles associating with lower viral loads and slower disease progression, certain CD8$^+$ T-cell responses restricted by these MHC-I molecules have been shown to be responsible for HIV control [11,12,13]. In rhesus macaque AIDS models, *Mamu-A*01*, *Mamu-B*08*, and *Mamu-B*17* are known as protective alleles, and macaques possessing these alleles tend to show slower disease progression after SIVmac251/SIVmac239 challenge [14,15,16,17].

Recent studies have indicated great contribution of CD8$^+$ T-cell responses targeting Gag epitopes to reduction in viral loads in HIV/SIV infection [18,19,20,21]. Viral control associated with some protective MHC-I alleles is attributed to Gag epitope-specific CD8$^+$ T-cell responses [22,23,24]. For instance, CD8$^+$ T-cell responses specific for the HLA-B*57-restricted $Gag_{240-249}$ TW10 and HLA-B*27-restricted $Gag_{263-272}$ KK10 epitopes exert strong suppressive pressure on HIV replication and frequently select for an escape mutation with viral fitness costs, leading to lower viral loads [22,24,25,26,27]. On the other hand, CD8$^+$ T-cell responses targeting SIV antigens other than Gag, such as Mamu-B*08- or Mamu-B*17-restricted Vif and Nef epitopes, have been indicated to exert strong suppressive pressure on SIV replication [28,29,30,31,32,33]. Accumulation of our knowledge on the potential of these non-Gag-specific as well as Gag-specific CD8$^+$ T-cell responses for HIV/SIV control should be encouraged for elucidation of viral control mechanisms.

We have been examining SIVmac239 infection in multiple groups of Burmese rhesus macaques sharing MHC-I genotypes at the haplotype level and indicated an association of MHC-I haplotypes with AIDS progression [21,34]. In our previous study, a group of macaques sharing MHC-I haplotype *90-120-Ia* (A) induced dominant Gag-specific $CD8^+$ T-cell responses and tended to show slower disease progression after SIVmac239 challenge [21]. Prophylactic immunization of these A^+ macaques with a DNA vaccine prime and a Gag-expressing Sendai virus (SeV-Gag) vector boost resulted in SIV control based on Gag-specific $CD8^+$

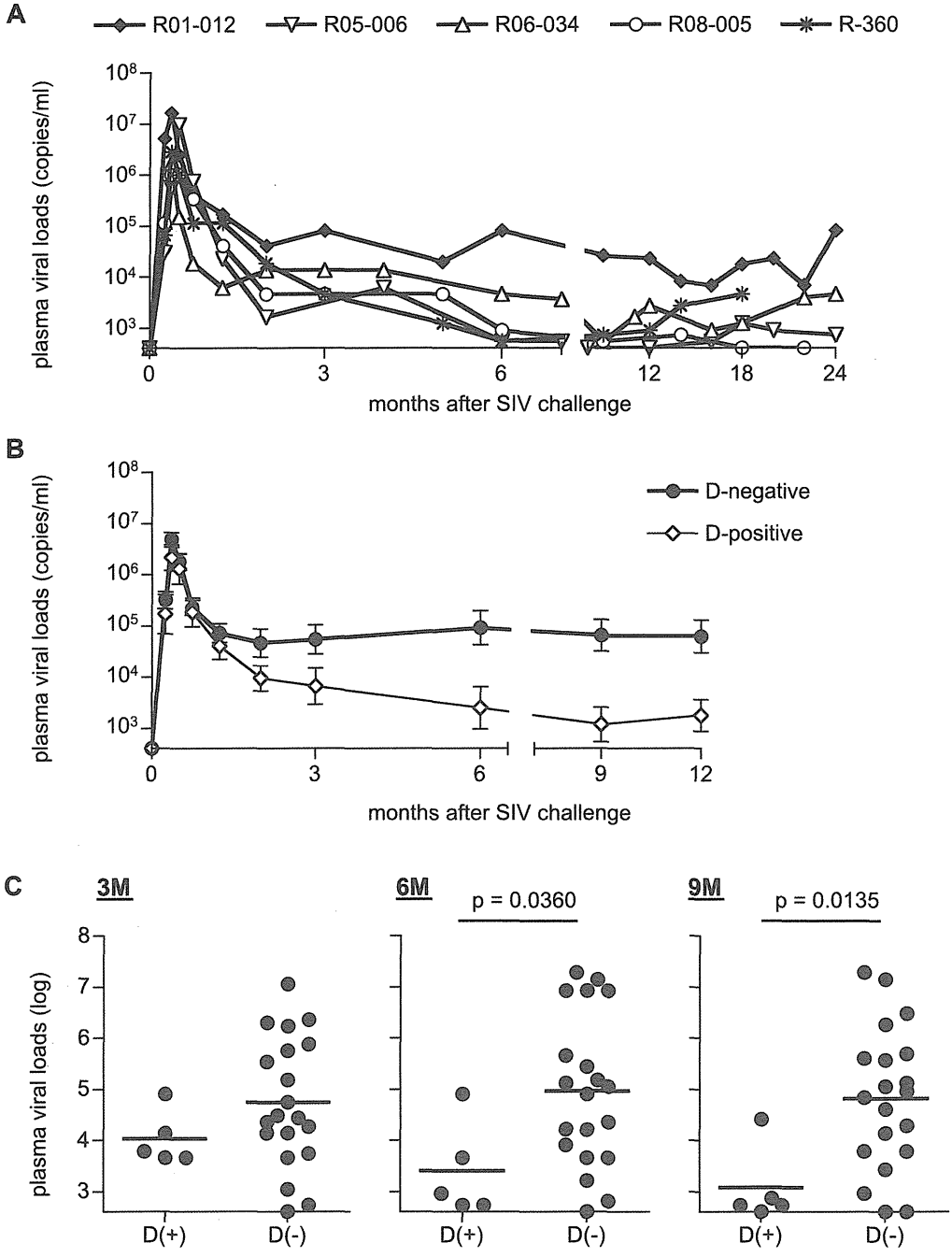

Figure 1. Plasma viral loads after SIVmac239 challenge in unvaccinated macaques. Plasma viral loads (SIV *gag* RNA copies/ml plasma) were determined as described previously [35]. The lower limit of detection is approximately 4×10^2 copies/ml. (A) Changes in plasma viral loads after challenge in unvaccinated macaques possessing MHC-I haplotype D. (B) Changes in geometric means of plasma viral loads after challenge in five unvaccinated D^+ animals in the present study and twenty D^- animals in our previous cohorts [21]. Three of twenty D^- animals were euthanized because of AIDS before 12 months, and we compared viral loads between D^+ and D^- animals until 12 months. (C) Comparison of plasma viral loads at 3 months (left panel), 6 months (middle panel), and 9 months (right panel) between the unvaccinated D^+ and the D^- animals. Viral loads at 6 months and 9 months in D^+ animals were significantly lower than those in the latter D^- animals ($p = 0.0360$ at 6 months and $p = 0.0135$ at 9 months by t-test).
doi:10.1371/journal.pone.0054300.g001

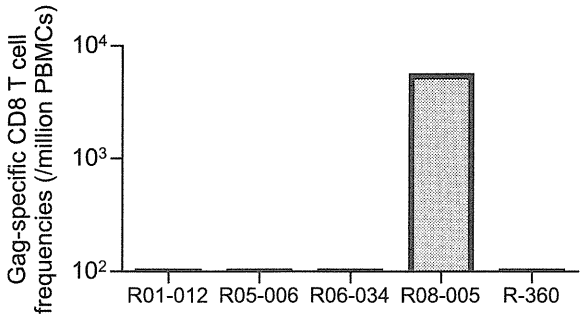

Figure 2. SIV Gag-specific CD8$^+$ T-cell responses in unvaccinated D$^+$ macaques at week 2 after SIVmac239 challenge.
doi:10.1371/journal.pone.0054300.g002

T-cell responses [35,36]. Accumulation of data on interaction between virus replication and T-cell responses in multiple groups of macaques sharing individual MHC-I haplotypes would provide great insights into our understanding of the mechanism for HIV/SIV control.

In the present study, we investigated SIVmac239 infection of a group of Burmese rhesus macaques possessing the MHC-I haplotype *90-010-Id* (D), which was not associated with dominant Gag-specific CD8$^+$ T-cell responses. These animals had persistent viremia in the early phase but showed significant reduction of viral loads around 6 months after SIV challenge. Most D$^+$ animals showed predominant Nef-specific but not Gag-specific CD8$^+$ T-cell responses. This study presents a protective MHC-I haplotype, indicating the potential of non-Gag antigen-specific CD8$^+$ T-cell responses to contribute to SIV control.

Materials and Methods

Ethics Statement

Animal experiments were carried out in National Institute of Biomedical Innovation (NIBP) and Institute for Virus Research in Kyoto University (IVRKU) after approval by the Committee on the Ethics of Animal Experiments of NIBP and IVRKU in accordance with the guidelines for animal experiments at NIBP, IVRKU, and National Institute of Infectious Diseases. To prevent viral transmission, animals were housed in individual cages allowing them to make sight and sound contact with one another, where the temperature was kept at 25°C with light in 12 hours per day. Animals were fed with apples and commercial monkey diet (Type CMK-2, Clea Japan, Inc. Tokyo). Blood collection, vaccination, and SIV challenge were performed under ketamine anesthesia. The endpoint for euthanasia was determined by typical signs of AIDS including reduction in peripheral CD4$^+$ T-cell counts (less than 200 cells/μl), 10% loss of body weight, diarrhea, and general weakness. At euthanasia, animals were deeply anesthetized with pentobarbital under ketamine anesthesia, and then, whole blood was collected from left ventricle.

Animal Experiments

We examined SIV infections in a group of Burmese rhesus macaques (n = 10) sharing the MHC-I haplotype *90-010-Id* (D). The determination of MHC-I haplotypes was based on the family study in combination with the reference strand-mediated conformation analysis (RSCA) of *Mamu-A* and *Mamu-B* genes and detection of major *Mamu-A* and *Mamu-B* alleles by cloning the reverse transcription (RT)-PCR products as described previously [21,34,37]. Macaques R01-012 and R01-009 used in our previous report [35] and macaques R03-021 and R03-016 used in an unpublished experiment were included in the present study. Five macaques R01-009, R06-020, R06-033, R03-021, and R03-016 received a prophylactic DNA prime/SeV-Gag boost vaccine (referred to as DNA/SeV-Gag vaccine) [35]. The DNA used for the vaccination, CMV-SHIVdEN, was constructed from an *env*-deleted and *nef*-deleted simian–human immunodeficiency virus SHIVMD14YE [38] molecular clone DNA (SIVGP1) and has the genes encoding SIVmac239 Gag, Pol, Vif, and Vpx, and HIV Tat and Rev. At the DNA vaccination, animals received 5 mg of CMV-SHIVdEN DNA intramuscularly. Six weeks after the DNA prime, animals received a single boost intranasally with 6×10^9 cell infectious units (CIUs) of F-deleted replication-defective SeV-Gag [39,40]. All animals were challenged intravenously with 1,000 $TCID_{50}$ (50 percent tissue culture infective doses) of SIVmac239 [41]. At week 1 after SIV challenge, macaque R03-021 was inoculated with nonspecific immunoglobulin G (IgG) and macaques R03-016 with IgG purified from neutralizing antibody-positive plasma of chronically SIV-infected macaques in our previous experiment [42].

Analysis of SIV Antigen-specific CD8$^+$ T-cell Responses

SIV antigen-specific CD8$^+$ T-cell responses were measured by flow-cytometric analysis of gamma interferon (IFN-γ) induction as described previously [43]. Autologous herpesvirus papio-immortalized B-lymphoblastoid cell lines (B-LCLs) were established from peripheral blood mononuclear cells (PBMCs) which were obtained from individual macaques before SIV challenge [44]. PBMCs obtained from SIV-infected macaques were cocultured with autologous B-LCLs pulsed with peptides or peptide pools using panels of overlapping peptides spanning the entire SIVmac239 Gag, Pol, Vif, Vpx, Vpr, Tat, Rev, Env, and Nef amino acid sequences. Alternatively, PBMCs were cocultured with B-LCLs infected with a vaccinia virus vector expressing SIVmac239 Gag for Gag-specific stimulation. Intracellular IFN-γ staining was performed using CytofixCytoperm kit (BD, Tokyo, Japan). Fluorescein isothiocianate-conjugated anti-human CD4 (BD), Peridinin chlorophyll protein (PerCP)-conjugated anti-human CD8 (BD), allophycocyanin Cy7 (APC-Cy7)-conjugated anti-human CD3 (BD), and phycoerythrin (PE)-conjugated anti-human IFN-γ antibodies (Biolegend, San Diego, CA) were used. Specific T-cell levels were calculated by subtracting non-specific IFN-γ$^+$ T-cell frequencies from those after peptide-specific stimulation. Specific T-cell levels less than 100 cells per million PBMCs were considered negative.

Sequencing Analysis of Plasma Viral Genomes

Viral RNAs were extracted using High Pure Viral RNA kit (Roche Diagnostics, Tokyo, Japan) from macaque plasma samples. Fragments of cDNAs encoding SIVmac239 Gag and Nef were amplified by nested RT-PCR from plasma RNAs and subjected to direct sequencing by using dye terminator chemistry and an automated DNA sequencer (Applied Biosystems, Tokyo, Japan) as described before [45]. Predominant non-synonymous mutations were determined.

Statistical Analysis

Statistical analysis was performed using Prism software version 4.03 with significance levels set at a P value of <0.050 (GraphPad Software, Inc., San Diego, CA). Plasma viral loads were log transformed and compared by an unpaired two-tailed t test.

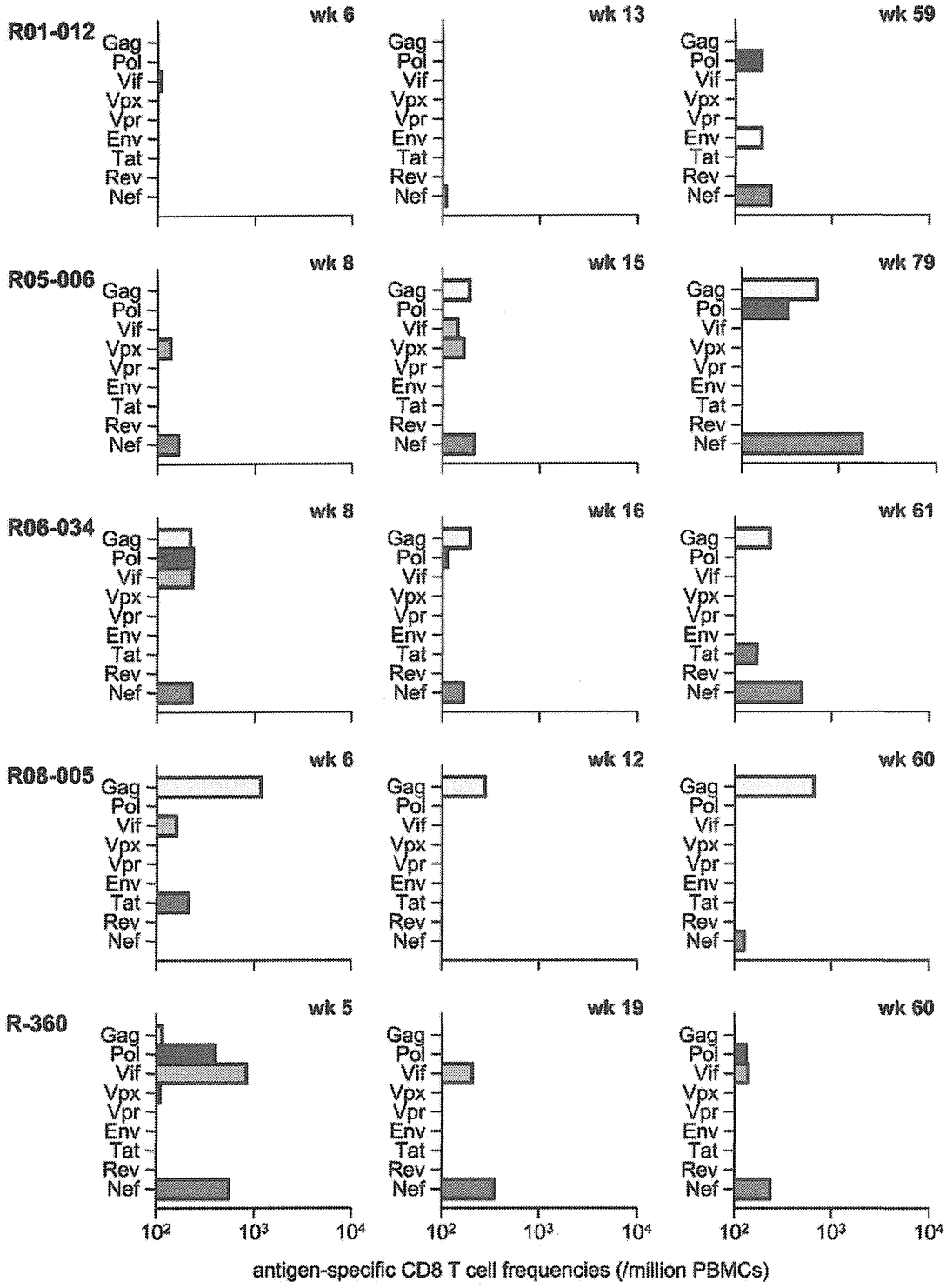

Figure 3. SIV antigen-specific CD8$^+$ T-cell responses in unvaccinated D$^+$ macaques. Responses were measured by the detection of antigen-specific IFN-γ induction in PBMCs obtained at indicated time points after SIVmac239 challenge.
doi:10.1371/journal.pone.0054300.g003

Results

Lower Viral Loads in D$^+$ Macaques in the Chronic Phase of SIV Infection

We first investigated SIVmac239 infection of five unvaccinated Burmese rhesus macaques sharing the MHC-I haplotype D (referred to as D$^+$ macaques). Confirmed MHC-I alleles consisting of this haplotype is *Mamu-A1*032:02*, *Mamu-B*004:01*, and *Mamu-B*102:01:01*. These animals showed lower set-point plasma viral loads (Fig. 1). Comparison of plasma viral loads between these five animals and our previous cohorts of SIVmac239-infected Burmese D-negative (D$^-$) rhesus macaques (n = 20) [21] revealed no

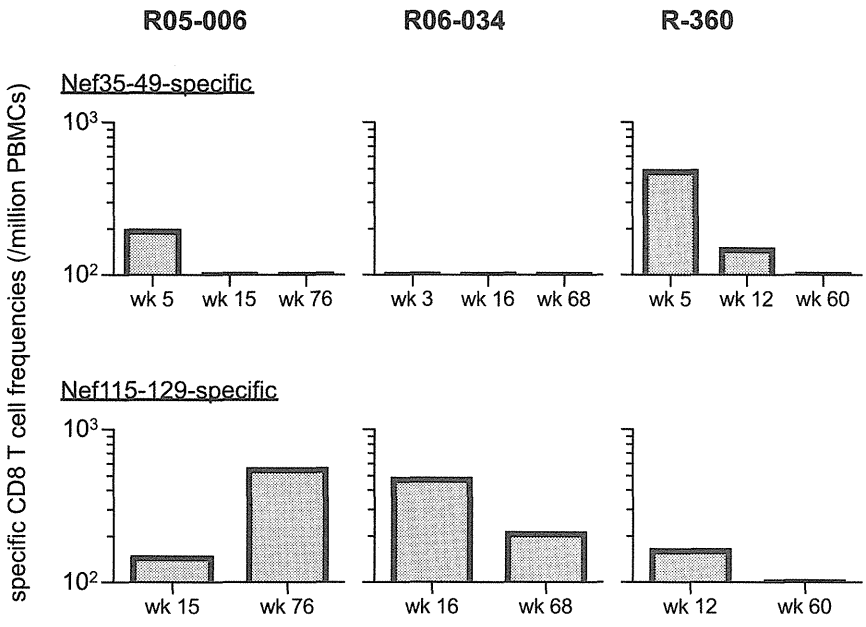

Figure 4. SIV Nef-specific CD8$^+$ T-cell responses in macaques R05-006, R06-034, and R-360. Nef_{35-49}-specific (upper panels) and $Nef_{115-129}$-specific (lower panels) CD8$^+$ T-cell responses were examined at indicated time points after SIVmac239 challenge.
doi:10.1371/journal.pone.0054300.g004

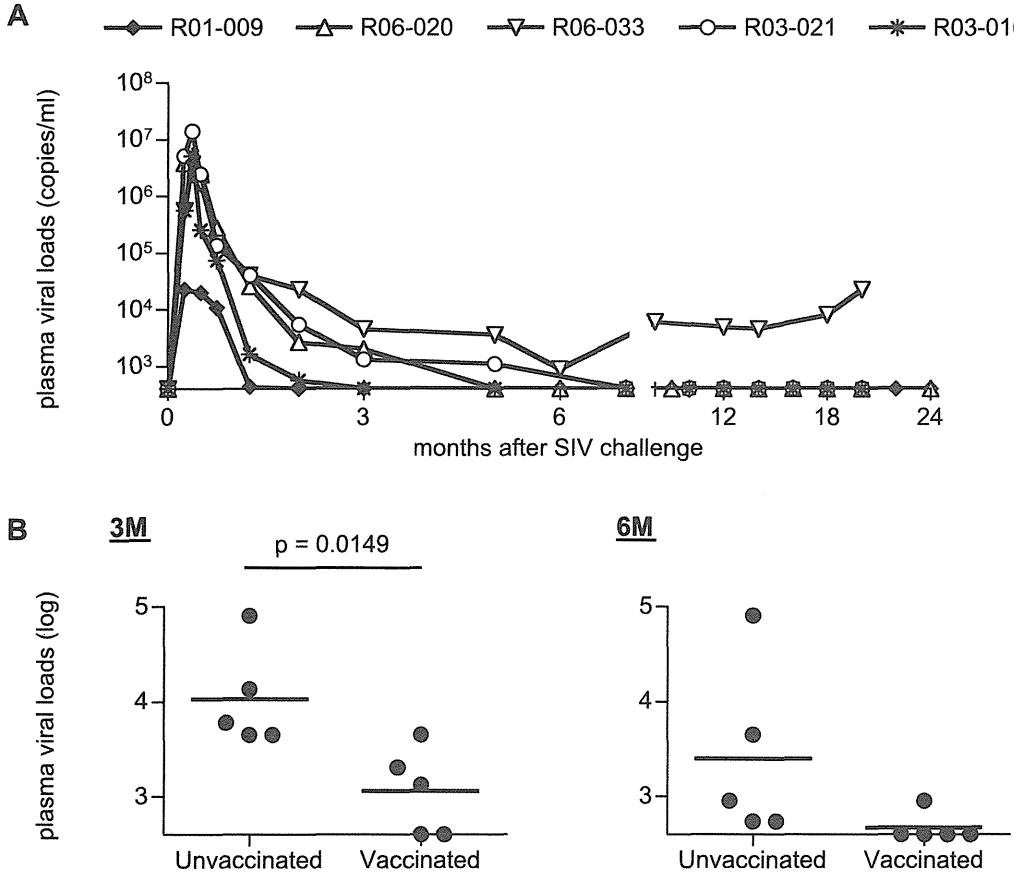

Figure 5. Plasma viral loads after SIVmac239 challenge in vaccinated D$^+$ macaques. (A) Changes in plasma viral loads after challenge vaccinated macaques possessing MHC-I haplotype D. (B) Comparison of plasma viral loads at 3 months (left panel) and 6 months (right panel) between five unvaccinated D$^+$ and five vaccinated D$^+$ animals. Viral loads at 3 months in vaccinated animals were significantly lower than those in the unvaccinated ($p = 0.0149$ by t-test).
doi:10.1371/journal.pone.0054300.g005

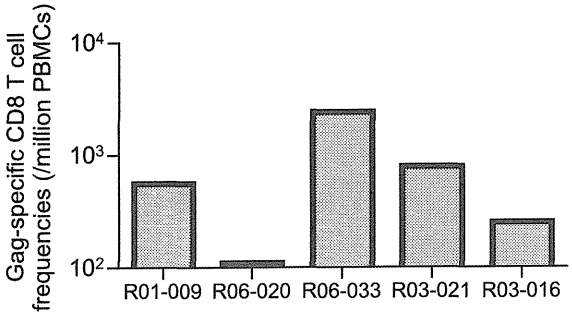

Figure 6. SIV Gag-specific CD8$^+$ T-cell responses in vaccinated D$^+$ macaques at week 2 after SIVmac239 challenge.
doi:10.1371/journal.pone.0054300.g006

significant difference at 3 months after SIV challenge ($p = 0.2436$ by t-test), but viral loads in the former D$^+$ animals became significantly lower than the latter after 6 months ($p = 0.0360$ at 6 months and $p = 0.0135$ at 9 months by t-test; Fig. 1). Four of these five macaques sharing MHC-I haplotype D showed low viral loads, less than 5×10^3 copies/ml, after 6 months, whereas macaque R01-012 maintained relatively higher viral loads.

Predominant Nef-specific CD8$^+$ T-cell Responses

We examined SIV antigen-specific CD8$^+$ T-cell responses by detection of antigen-specific IFN-γ induction. In the very acute phase, we did not have enough PBMC samples for measurement of individual SIV antigen-specific CD8$^+$ T-cell responses and focused on examining Gag-specific CD8$^+$ T-cell responses in most animals. At week 2 after challenge, Gag-specific CD8$^+$ T-cell responses were undetectable in four of five animals (Fig. 2).

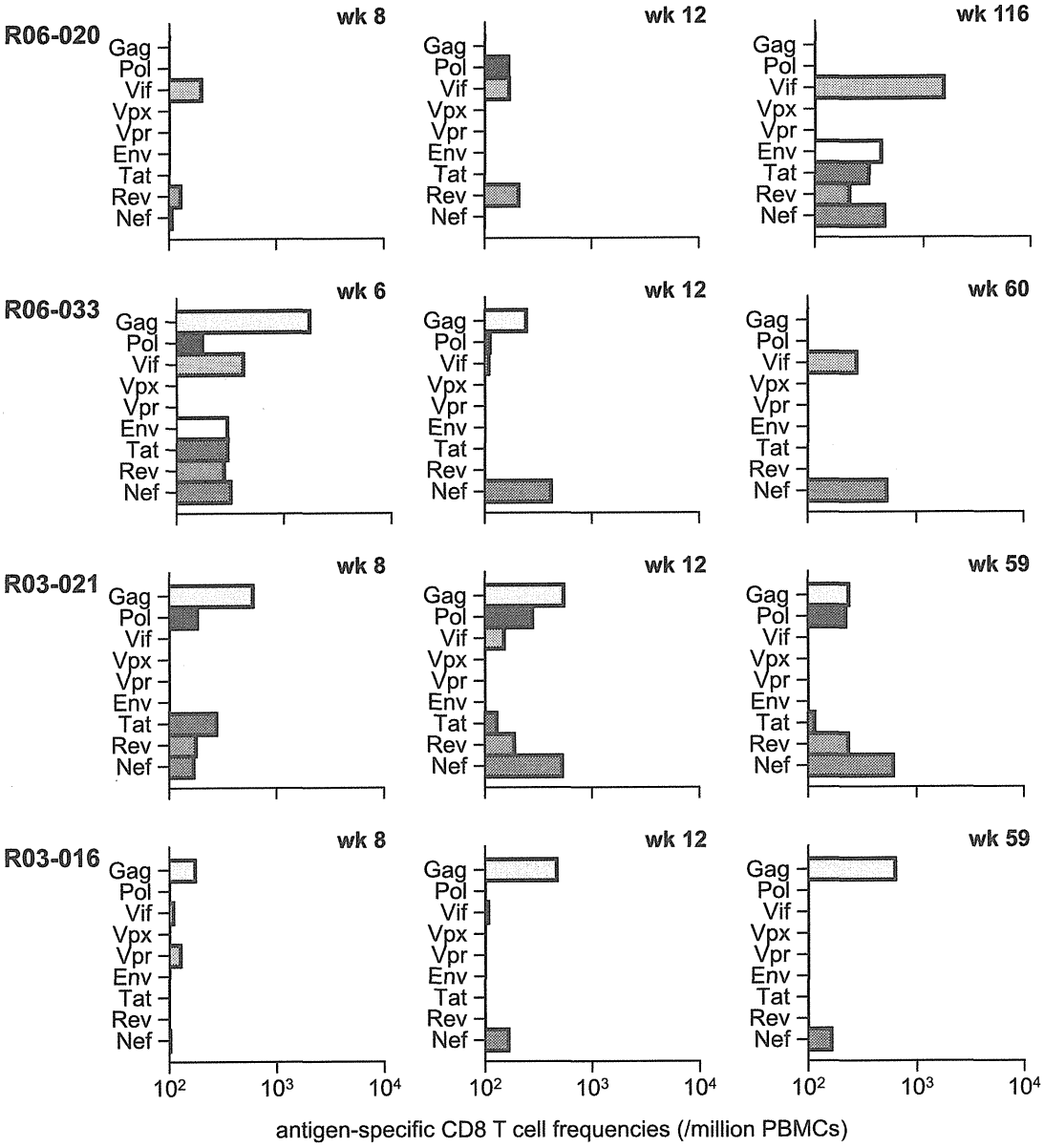

Figure 7. SIV antigen-specific CD8$^+$ T-cell responses in vaccinated D$^+$ animals after SIVmac239 challenge. Samples for this analysis were unavailable in macaque R01-009.
doi:10.1371/journal.pone.0054300.g007

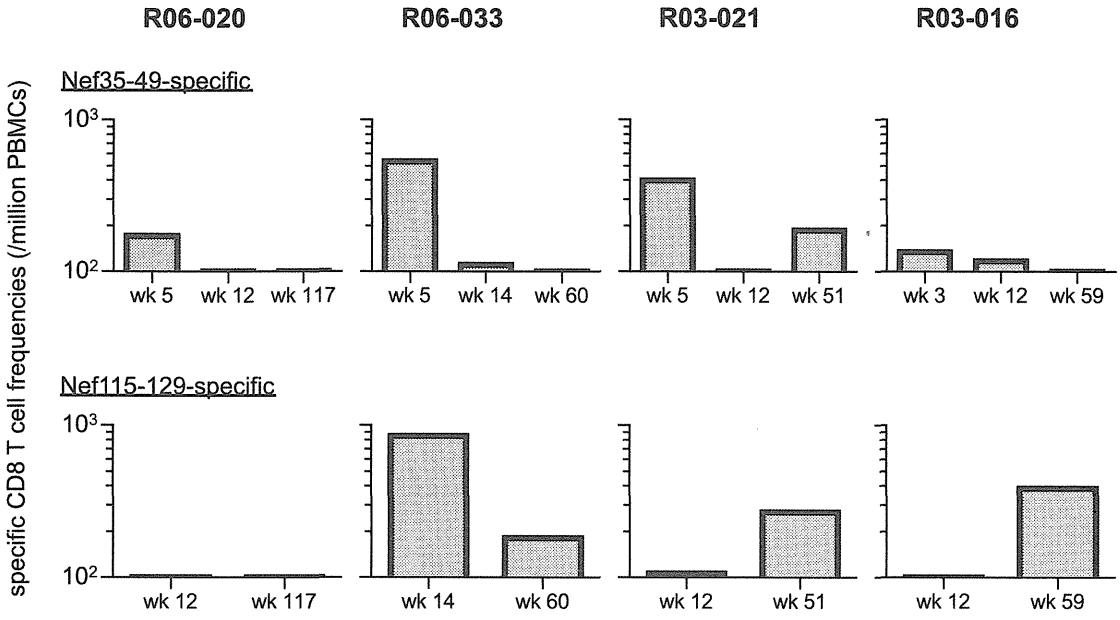

Figure 8. SIV Nef-specific CD8$^+$ T-cell responses in macaques R06-020, R06-033, R03-021, and R03-016. Nef_{35-49}-specific (upper panels) and $Nef_{115-129}$-specific (lower panels) CD8$^+$ T-cell responses were examined at indicated time points after SIVmac239 challenge.
doi:10.1371/journal.pone.0054300.g008

We then examined CD8$^+$ T-cell responses specific for individual SIV antigens in the early and the late phases (Fig. 3). Nef-specific but not Gag-specific CD8$^+$ T-cell responses were predominant in most D$^+$ animals. Gag-specific CD8$^+$ T-cell responses were dominantly induced in macaque R08-005 showing very low set-point viral loads. Macaque R01-012 having higher viral loads showed poor CD8$^+$ T-cell responses in the early phase.

Among four D$^+$ animals controlling SIV replication with less than 5×10^3 copies/ml of plasma viral loads after 6 months, Gag-specific CD8$^+$ T-cell responses were dominant only in macaque R08-005, while efficient Nef-specific CD8$^+$ T-cell responses were induced in the remaining three, suggesting possible contribution of Nef-specific CD8$^+$ T-cell responses to SIV control in these three controllers (R05-006, R06-034, and R-360). We then attempted to localize Nef CD8$^+$ T-cell epitopes shared in these animals and found Nef_{35-49}-specific and $Nef_{115-129}$-specific CD8$^+$ T-cell responses (Fig. 4), although we did not have enough samples for mapping the exact epitopes.

Reduction of Viral Loads in the Early Phase of SIV Infection by Prophylactic Vaccination

We also investigated SIVmac239 infection of additional five, vaccinated Burmese rhesus macaques sharing the MHC-I haplotype D. These animals received a prophylactic DNA/SeV-Gag vaccination. In four of these five vaccinated macaques, plasma viremia became undetectable after 6 months, while macaque R06-033 showed persistent viremia (Fig. 5A). Difference in viral loads between unvaccinated and vaccinated D$^+$ animals was unclear in the acute phase, but the latter vaccinees showed significant reduction in viral loads compared to those in the former unvaccinated at 3 months ($p = 0.0360$; Fig. 5B). After 6 months, unvaccinated animals also showed reduced viral loads, and the difference in viral loads between unvaccinated and vaccinated became unclear.

In contrast to unvaccinated D$^+$ animals, all five vaccinated animals elicited Gag-specific CD8$^+$ T-cell responses at week 2 after challenge (Fig. 6), reflecting the effect of prophylactic vaccination. We then examined CD8$^+$ T-cell responses specific for individual SIV antigens in these vaccinated animals (Fig. 7). Samples for this analysis were unavailable in vaccinated macaque R01-009. Vaccinated animals except for macaque R06-020 showed dominant Gag-specific CD8$^+$ T-cell responses even at 1–2 months. However, Gag-specific CD8$^+$ T-cell responses became not dominant after 1 year, while Nef-specific or Vif-specific CD8$^+$ T-cell responses became predominant, instead, in most vaccinees except for macaque R03-016.

Like three unvaccinated macaques (R05-006, R06-034, and R-360), vaccinated D$^+$ animals induced Nef_{35-49}-specific and $Nef_{115-129}$-specific CD8$^+$ T-cell responses after SIV challenge (Fig. 8). In analyses of three unvaccinated (Fig. 4) and four vaccinated animals (Fig. 8), Nef_{35-49}-specific CD8$^+$ T-cell responses were induced in the early phase in six animals but mostly became undetectable in the chronic phase. $Nef_{115-129}$-specific CD8$^+$ T-cell responses were also induced in most animals except for macaque R06-020 which showed $Nef_{112-126}$-specific ones in the chronic phase (data not shown). Macaques R05-006, R03-021, and R03-016 showed efficient $Nef_{115-129}$-specific CD8$^+$ T-cell responses not in the early phase but in the chronic phase. In contrast, vaccinated animal R06-033 that failed to control viremia showed higher $Nef_{115-129}$-specific CD8$^+$ T-cell responses in the early phase than those in the chronic phase.

Selection of Mutations in Nef CD8$^+$ T-cell Epitope-coding Regions

To see the effect of selective pressure by Nef-specific CD8$^+$ T-cell responses on viral genome mutations, we next analyzed nucleotide sequences in viral *nef* cDNAs amplified from plasma RNAs obtained at several time points after SIV challenge. Nonsynonymous mutations detected predominantly in Nef_{35-49}-coding and $Nef_{115-129}$-coding regions were as shown in Fig. 9. Remarkably, all the unvaccinated and vaccinated D$^+$ animals showed rapid selection of mutations in the Nef_{35-49}-coding region in 3 months. On the other hand, mutations in the $Nef_{115-129}$-coding region were observed in the late phase in all the three

		Nef35-49						Nef115-129				
Nef		36	37	41	42	44		119	122	124	125	126
		E	D	Q	S	G		M	F	K	E	K
R01-012	1M		*G									
	3M		*G									
	14M	*G	*G									
	24M	*G	*G			*E						
R05-006	1M					*E						
	3M			R								
	16M			R								
	24M			R								R
R06-034	1M											
	3M	*G										
	10M	*G	*G			*E						*R
	18M	G				E						R
R08-005	1M											
	3M				*F							
	6M	G										
	14M				F							
	24M	*G			F							
R-360	1M											
	3M		*G									
	6M		G									
	12M		G					T	L			
	20M		G					T	L			
R06-020	1M											
	3M	*K										
	11M		G	R								
R06-033	1M											
	3M	*G										
	6M		*G									
	14M		G			*E					K	E
R03-021	1M											
	3M				*F							
	14M	G								R		
R03-016	1M	*K		*R								
	4M	K										
	12M	K										

Figure 9. Predominant non-synonymous mutations in Nef_{35-49}-coding and $Nef_{115-129}$-coding regions of viral cDNAs in D^+ animals after SIVmac239 challenge. Amino acid substitutions are shown. Detection of similar levels of wild-type and mutant sequences at the residue is indicated by asterisks. Samples for this analysis were unavailable in macaque R01-009.
doi:10.1371/journal.pone.0054300.g009

unvaccinated animals eliciting $Nef_{115-129}$-specific $CD8^+$ T-cell responses. These mutations were also detected in two of three vaccinated animals eliciting $Nef_{115-129}$-specific $CD8^+$ T-cell responses.

We also analyzed viral *gag* sequences to see the effect of Gag-specific $CD8^+$ T-cell pressure on viral genome mutations in vaccinated animals (data not shown). Our previous study [35] showed rapid selection of a mutation leading to a glutamine (Q)-to-lysine (K) change at the 58th residue in Gag (Q58K) at week 5 in vaccinated macaque R01-009, although no more samples were available for this sequencing analysis. This Q58K mutation results in escape from Gag_{50-65}-specific $CD8^+$ T-cell recognition. In the present study, macaque R03-016 showed rapid selection of a mutation leading to a K-to-asparagine (N) change at the 478th residue in Gag in 1 month. These results may reflect rapid disappearance of detectable plasma viremia in 1 or 2 months in these two vaccinees. Macaque R06-020 showed selection of a *gag* mutation in 3 months, while other two vaccinees (R06-033 and R03-021) selected no *gag* mutation in the early phase.

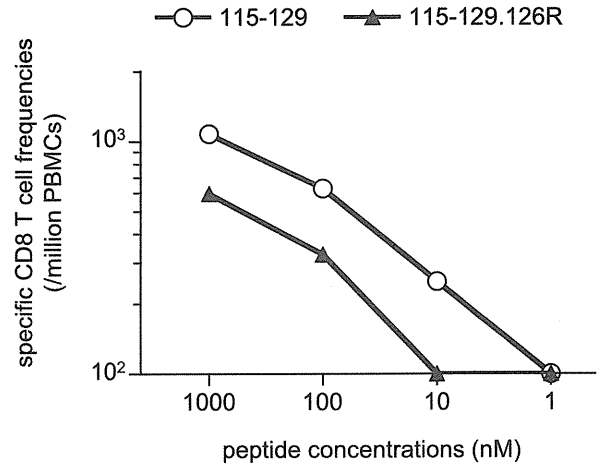

Figure 10. IFN-γ induction in $CD8^+$ T cells after stimulation with the wild-type or the mutant peptide. PBMCs obtained at week 31 from macaque R06-033 were stimulated by coculture with B-LCL pulsed with indicated concentrations of the wild-type $Nef_{115-129}$ peptide (open circles, 115–129, LAIDMSHFIKEKGGL) or the mutant $Nef_{115-129}$ peptide with a K126R alteration (closed triangles, 115–129.126R, LAIDMSHFIKERGGL).
doi:10.1371/journal.pone.0054300.g010

Discussion

HIV infection in humans with polymorphic MHC-I genotypes induces various patterns of viral antigen-specific $CD8^+$ T-cell responses. Previous studies have found several protective MHC-I alleles associated with lower viral loads and slower disease progression in HIV/SIV infection [7,13,14,16,17]. Elucidation of the mechanisms of viral control associated with individual protective MHC-I alleles would contribute to HIV cure and vaccine-based prevention. Because $CD8^+$ T-cell responses specific for some MHC-I-restricted epitopes can be affected by those specific for other MHC-I-restricted epitopes due to immunodominance [29,46,47], macaque groups sharing MHC-I genotypes at the haplotype level are useful for the analysis of cooperation of multiple epitope-specific $CD8^+$ T-cell responses. Previously, we reported a group of Burmese rhesus macaques sharing MHC-I haplotype *90-120-Ia* (A), which dominantly induce Gag-specific $CD8^+$ T-cell responses and tend to show slower disease progression after SIVmac239 challenge [21]. In the present study, we presented another type of protective MHC-I haplotype, which is not associated with dominant Gag-specific $CD8^+$ T-cell responses. Significant reduction of viral loads in unvaccinated macaques possessing this D haplotype compared to those in D^- macaques was observed after 6 months. Analysis of SIV infection in macaques sharing this protective MHC-I haplotype would lead to understanding of $CD8^+$ T-cell cooperation for viral control.

Analyses of antigen-specific $CD8^+$ T-cell responses after SIVmac239 challenge indicate that this MHC-I haplotype D is associated with predominant Nef-specific $CD8^+$ T-cell responses. Nef-specific $CD8^+$ T-cell responses were efficiently induced in all SIV controllers, whereas Gag-specific $CD8^+$ T-cell responses were dominant in only one of them. We found Nef_{35-49}-specific and $Nef_{115-129}$-specific $CD8^+$ T-cell responses shared in D^+ animals. We were unable to determine the MHC-I alleles restricting these epitopes, but these responses are not usually induced in our

previous D^- cohorts and considered to be associated with this MHC-I haplotype D.

Sequencing analysis of viral genomes showed rapid selection of mutations in the Nef_{36-44}-coding region within 3 months in all the D^+ animals. This is consistent with our results that Nef_{35-49}-specific $CD8^+$ T-cell responses were mostly induced in the early phase but undetectable in the chronic phase. These mutations were not consistently selected in our previous D^- cohorts and thus considered as MHC-I haplotype D-associated mutations. This suggests strong selective pressure by Nef_{35-49}-specific $CD8^+$ T-cell responses in the acute phase of SIVmac239 infection in D^+ macaques, although it remains undetermined whether these mutations result in viral escape from Nef_{35-49}-specific $CD8^+$ T-cell recognition.

$Nef_{115-129}$-specific $CD8^+$ T-cell responses were detected in six D^+ animals. In five of them, nonsynonymous mutations in the $Nef_{119-126}$-coding region were observed in the chronic phase. At least, we confirmed viral escape from $Nef_{115-129}$-specific $CD8^+$ T-cell recognition by a mutation leading to a K-to-arginine (R) (K126R) substitution at Nef residue 126 (Fig. 10). The number of nonsynonymous substitutions per the number of sites estimated to be nonsynonymous (dN) exceeded that estimated to be synonymous (dS) during the evolution process of $Nef_{115-129}$-coding region, but the value did not show statistically significant difference from that of neutral selection. Among three unvaccinated animals that controlled SIV replication without dominant Gag-specific $CD8^+$ T-cell responses, amino acid substitutions in the $Nef_{119-126}$-coding region were observed in a year in macaques R06-034 and R-360 but after 2 years in macaque R05-006. The former two animals tended to show earlier increases in plasma viral loads in the chronic phase, while the latter R05-006 maintained higher frequencies of $Nef_{115-129}$-specific $CD8^+$ T-cell responses. $Nef_{115-129}$-specific $CD8^+$ T-cell responses were efficient in the chronic phase in vaccinated controllers R03-021 and R03-016 but decreased in R06-033 that failed to contain SIV replication. Although a possible effect of this haplotype-associated factors other than $CD8^+$ T-cell responses such as NK activity on SIV infection [48,49,50] remains undetermined, these results imply involvement of Nef-specific $CD8^+$ T-cell responses in the SIV control associated with MHC-I haplotype D.

Unvaccinated macaque R08-005 dominantly elicited Gag antigen-specific $CD8^+$ T-cell responses and showed rapid selection of a mutation encoding Gag 257 residue, which was not observed in any other D^+ animals. Nef-specific $CD8^+$ T-cell responses were detectable only at week 2 in the acute phase (data not shown) and a mutation in the Nef_{42}-coding region was rapidly selected. It is speculated that those dominant Gag-specific $CD8^+$ T-cell responses associated with the second, non-D MHC-I haplotype were effective in this animal. Nef_{35-49}-specific $CD8^+$ T-cell responses may not be efficient due to immunodominance but exert some suppressive pressure on viral replication.

DNA/SeV-Gag vaccination resulted in earlier reduction of viral loads after SIV challenge. Vaccinees showed significantly lower viral loads at 3 months than those in unvaccinated animals. Gag-specific $CD8^+$ T-cell responses were elicited at week 2 in all the vaccinees but not in the unvaccinated except for one animal R08-005. No *gag* mutations were shared in the vaccinees in the acute phase, but three of them showed rapid selection of individual non-synonymous mutations in *gag*. Rapid selection of mutations in the Nef_{36-44}-coding region was consistently detected even in these vaccinees. These results suggest broader $CD8^+$ T-cell responses consisting of dominant vaccine antigen Gag-specific and inefficient naive-derived Nef-specific ones in the acute phase. In three vaccinated animals, Gag-specific $CD8^+$ T-cell responses became lower or undetectable, and instead, Nef-specific $CD8^+$ T-cell responses became predominant in the chronic phase.

In summary, we found a protective MHC-I haplotype not associated with dominant Gag-specific $CD8^+$ T-cell responses in SIVmac239 infection. Our results in D^+ macaques suggest suppressive pressure by Nef_{35-49}-specific and $Nef_{115-129}$-specific $CD8^+$ T-cell responses on SIV replication, contributing to reduction in set-point viral loads. DNA/SeV-Gag-vaccinated D^+ animals induced Gag-specific $CD8^+$ T-cell responses in addition to Nef-specific ones after SIV challenge, resulting in earlier containment of SIV replication. This study presents a pattern of SIV control with involvement of non-Gag antigen-specific $CD8^+$ T-cell responses, contributing to accumulation of our knowledge on HIV/SIV control mechanisms.

Acknowledgments

We thank F. Ono, K. Oto, K. Hanari, K. Komatsuzaki, M. Hamano, H. Akari, and Y. Yasutomi for their assistance in animal experiments.

Author Contributions

Performed animal experiments: HS TM TI YK. Performed MHC-I typing: TKN AK. Conceived and designed the experiments: NT TM. Performed the experiments: NT TN YT HY AT. Analyzed the data: NT HY T. Shiino TM. Contributed reagents/materials/analysis tools: MI AI HH T. Shu MH. Wrote the paper: NT TM.

References

1. Borrow P, Lewicki H, Hahn BH, Shaw GM, Oldstone MB (1994) Virus-specific CD8+ cytotoxic T-lymphocyte activity associated with control of viremia in primary human immunodeficiency virus type 1 infection. J Virol 68: 6103–6110.
2. Koup RA, Safrit JT, Cao Y, Andrews CA, McLeod G, et al. (1994) Temporal association of cellular immune responses with the initial control of viremia in primary human immunodeficiency virus type 1 syndrome. J Virol 68: 4650–4655.
3. Matano T, Shibata R, Siemon C, Connors M, Lane HC, et al. (1998) Administration of an anti-CD8 monoclonal antibody interferes with the clearance of chimeric simian/human immunodeficiency virus during primary infections of rhesus macaques. J Virol 72: 164–169.
4. Jin X, Bauer DE, Tuttleton SE, Lewin S, Gettie A, et al. (1999) Dramatic rise in plasma viremia after CD8+ T cell depletion in simian immunodeficiency virus-infected macaques. J Exp Med 189: 991–998.
5. Schmitz JE, Kuroda MJ, Santra S, Sasseville VG, Simon MA, et al. (1999) Control of viremia in simian immunodeficiency virus infection by CD8+ lymphocytes. Science 283: 857–860.
6. Carrington M, Nelson GW, Martin MP, Kissner T, Vlahov D, et al. (1999) HLA and HIV-1: heterozygote advantage and B*35-Cw*04 disadvantage. Science 283: 1748–1752.
7. Migueles SA, Sabbaghian MS, Shupert WL, Bettinotti MP, Marincola FM, et al. (2000) HLA B*5701 is highly associated with restriction of virus replication in a subgroup of HIV-infected long term nonprogressors. Proc Natl Acad Sci USA 97: 2709–2714.
8. Tang J, Tang S, Lobashevsky E, Myracle AD, Fideli U, et al. (2002) Favorable and unfavorable HLA class I alleles and haplotypes in Zambians predominantly infected with clade C human im- munodeficiency virus type 1. J Virol 76: 8276–8284.
9. Kiepiela P, Leslie AJ, Honeyborne I, Ramduth D, Thobakgale C, et al. (2004) Dominant influence of HLA-B in mediating the potential co-evolution of HIV and HLA. Nature 432: 769–775.
10. Leslie A, Matthews PC, Listgarten J, Carlson JM, Kadie C, et al. (2010) Additive contribution of HLA class I alleles in the immune control of HIV-1 infection. J Virol 84: 9879–9888.
11. Altfeld M, Addo MM, Rosenberg ES, Hecht FM, Lee PK, et al. (2003) Influence of HLA-B57 on clinical presentation and viral control during acute HIV-1 infection. AIDS 17: 2581–2591.
12. Altfeld M, Kalife ET, Qi Y, Streeck H, Lichterfeld M, et al. (2006) HLA alleles associated with delayed progression to AIDS contribute strongly to the initial CD8+ T cell response against HIV-1. PLoS Med 3: e403.
13. Goulder PJ, Watkins DI (2008) Impact of MHC class I diversity on immune control of immunodeficiency virus replication. Nat Rev Immunol 8: 619–630.

14. Muhl T, Krawczak M, Ten Haaft P, Hunsmann G, Sauermann U (2002) MHC class I alleles influence set-point viral load and survival time in simian immunodeficiency virus-infected rhesus monkeys. J Immunol 169: 3438–3446.
15. Mothe BR, Weinfurter J, Wang C, Rehrauer W, Wilson N, et al. (2003) Expression of the major histocompatibility complex class I molecule Mamu-A*01 is associated with control of simian immunodeficiency virus SIVmac239 replication. J Virol 77: 2736–2740.
16. Yant LJ, Friedrich TC, Johnson RC, May GE, Maness NJ, et al. (2006) The high-frequency major histocompatibility complex class I allele Mamu-B*17 is associated with control of simian immunodeficiency virus SIVmac239 replication. J Virol 80: 5074–5077.
17. Loffredo JT, Maxwell J, Qi Y, Glidden CE, Borchardt GJ, et al. (2007) Mamu-B*08-positive macaques control simian immunodeficiency virus replication. J Virol 81: 8827–8832.
18. Edwards BH, Bansal A, Sabbaj S, Bakari J, Mulligan MJ, et al. (2002) Magnitude of functional CD8+ T-cell responses to the gag protein of human immunodeficiency virus type 1 correlates inversely with viral load in plasma. J Virol 76: 2298–2305.
19. Zuniga R, Lucchetti A, Galvan P, Sanchez S, Sanchez C, et al. (2006) Relative dominance of Gag p24-specific cytotoxic T lymphocytes is associated with human immunodeficiency virus control. J Virol 80: 3122–3125.
20. Kiepiela P, Ngumbela K, Thobakgale C, Ramduth D, Honeyborne I, et al. (2007) CD8+ T-cell responses to different HIV proteins have discordant associations with viral load. Nat Med 13: 46–53.
21. Nomura T, Yamamoto H, Shiino T, Takahashi N, Nakane T, et al. (2012) Association of major histocompatibility complex class I haplotypes with disease progression after simian immunodeficiency virus challenge in Burmese rhesus macaques. J Virol 86: 6481–6490.
22. Schneidewind A, Brockman MA, Yang R, Adam RI, Li B, et al. (2007) Escape from the dominant HLA-B27-restricted cytotoxic T-lymphocyte response in Gag is associated with a dramatic reduction in human immunodeficiency virus type 1 replication. J Virol 81: 12382–12393.
23. Emu B, Sinclair E, Hatano H, Ferre A, Shacklett B, et al. (2008) HLA class I-restricted T-cell responses may contribute to the control of human immunodeficiency virus infection, but such responses are not always necessary for long-term virus control. J Virol 82: 5398–5407.
24. Miura T, Brockman MA, Schneidewind A, Lobritz M, Pereyra F, et al. (2009) HLA-B57/B*5801 human immunodeficiency virus type 1 elite controllers select for rare gag variants associated with reduced viral replication capacity and strong cytotoxic T-lymphocyte recognition. J Virol 83: 2743–2755.
25. Leslie AJ, Pfafferott KJ, Chetty P, Draenert R, Addo MM, et al. (2004) HIV evolution: CTL escape mutation and reversion after transmission. Nat Med 10: 282–289.
26. Martinez-Picado J, Prado JG, Fry EE, Pfafferott K, Leslie A, et al. (2006) Fitness cost of escape mutations in p24 Gag in association with control of human immunodeficiency virus type 1. J Virol 80: 3617–3623.
27. Crawford H, Prado JG, Leslie A, Hue S, Honeyborne I, et al. (2007) Compensatory mutation partially restores fitness and delays reversion of escape mutation within the immunodominant HLA-B*5703-restricted Gag epitope in chronic human immunodeficiency virus type 1 infection. J Virol 81: 8346–8351.
28. Friedrich TC, Valentine LE, Yant LJ, Rakasz EG, Piaskowski SM, et al. (2007) Subdominant CD8+ T-cell responses are involved in durable control of AIDS virus replication. J Virol 81: 3465–3476.
29. Loffredo JT, Bean AT, Beal DR, Leon EJ, May GE, et al. (2008) Patterns of CD8+ immunodominance may influence the ability of Mamu-B*08-positive macaques to naturally control simian immunodeficiency virus SIVmac239 replication. J Virol 82: 1723–1738.
30. Maness NJ, Yant LJ, Chung C, Loffredo JT, Friedrich TC, et al. (2008) Comprehensive immunological evaluation reveals surprisingly few differences between elite controller and progressor Mamu-B*17-positive simian immunodeficiency virus-infected rhesus macaques. J Virol 82: 5245–5254.
31. Valentine LE, Loffredo JT, Bean AT, Leon EJ, MacNair CE, et al. (2009) Infection with "escaped" virus variants impairs control of simian immunodeficiency virus SIVmac239 replication in Mamu-B*08-positive macaques. J Virol 83: 11514–11527.
32. Budde ML, Greene JM, Chin EN, Ericsen AJ, Scarlotta M, et al. (2012) Specific CD8+ T cell responses correlate with control of simian immunodeficiency virus replication in Mauritian cynomolgus macaques. J Virol 86: 7596–7604.
33. Mudd PA, Martins MA, Ericsen AJ, Tully DC, Power KA, et al. (2012) Vaccine-induced CD8+ T cells control AIDS virus replication. Nature 491: 129–133.
34. Naruse TK, Chen Z, Yanagida R, Yamashita T, Saito Y, et al. (2010) Diversity of MHC class I genes in Burmese-origin rhesus macaques. Immunogenetics 62: 601–611.
35. Matano T, Kobayashi M, Igarashi H, Takeda A, Nakamura H, et al. (2004) Cytotoxic T lymphocyte-based control of simian immunodeficiency virus replication in a preclinical AIDS vaccine trial. J Exp Med 199: 1709–1718.
36. Kawada M, Tsukamoto T, Yamamoto H, Iwamoto N, Kurihara K, et al. (2008) Gag-specific cytotoxic T-lymphocyte-based control of primary simian immunodeficiency virus replication in a vaccine trial. J Virol 82: 10199–10206.
37. Tanaka-Takahashi Y, Yasunami M, Naruse T, Hinohara K, Matano T, et al. (2007) Reference strand-mediated conformation analysis-based typing of multiple alleles in the rhesus macaque MHC class I Mamu-A and Mamu-B loci. Electrophoresis 28: 918–924.
38. Shibata R, Maldarelli F, Siemon C, Matano T, Parta M, et al. (1997) Infection and pathogenicity of chimeric simian-human immunodeficiency viruses in macaques: determinants of high virus loads and CD4 cell killing. J Infect Dis 176: 362–373.
39. Li HO, Zhu YF, Asakawa M, Kuma H, Hirata T, et al. (2000) A cytoplasmic RNA vector derived from nontransmissible Sendai virus with efficient gene transfer and expression. J Virol 74: 6564–6569.
40. Takeda A, Igarashi H, Nakamura H, Kano M, Iida A, et al. (2003) Protective efficacy of an AIDS vaccine, a single DNA priming followed by a single booster with a recombinant replication-defective Sendai virus vector, in a macaque AIDS model. J Virol 77: 9710–9715.
41. Kestler HW III, Ringler DJ, Mori K, Panicali DL, Sehgal PK, et al. (1991) Importance of the nef gene for maintenance of high virus loads and for development of AIDS. Cell 65: 651–662.
42. Yamamoto H, Kawada M, Takeda A, Igarashi H, Matano T (2007) Post-infection immunodeficiency virus control by neutralizing antibodies. PLoS One 2: e540.
43. Iwamoto N, Tsukamoto T, Kawada M, Takeda A, Yamamoto H, et al. (2010) Broadening of CD8+ cell responses in vaccine-based simian immunodeficiency virus controllers. AIDS 24: 2777–2787.
44. Voss G, Nick S, Stahl-Hennig C, Ritter K, Hunsmann G (1992) Generation of macaque B lymphoblastoid cell lines with simian Epstein-Barr-like viruses: transformation procedure, characterization of the cell lines and occurrence of simian foamy virus. J Virol Methods 39: 185–195.
45. Kawada M, Igarashi H, Takeda A, Tsukamoto T, Yamamoto H, et al. (2006) Involvement of multiple epitope-specific cytotoxic T-lymphocyte responses in vaccine-based control of simian immunodeficiency virus replication in rhesus macaques. J Virol 80: 1949–1958.
46. Tenzer S, Wee E, Burgevin A, Stewart-Jones G, Friis L, et al. (2009) Antigen processing influences HIV-specific cytotoxic T lymphocyte immunodominance. Nat Immunol 10: 636–646.
47. Ishii H, Kawada M, Tsukamoto T, Yamamoto H, Matsuoka S, et al. (2012) Impact of vaccination on cytotoxic T lymphocyte immunodominance and cooperation against simian immunodeficiency virus replication in rhesus macaques. J Virol 86: 738–745.
48. Flores-Villanueva PO, Yunis EJ, Delgado JC, Vittinghoff E, Buchbinder S, et al. (2001) Control of HIV-1 viremia and protection from AIDS are associated with HLA-Bw4 homozygosity. Proc Natl Acad Sci USA 98: 5140–5145.
49. Martin MP, Gao X, Lee JH, Nelson GW, Detels R, et al. (2002) Epistatic interaction between KIR3DS1 and HLA-B delays the progression to AIDS. Nat Genet 31: 429–434.
50. Martin MP, Qi Y, Gao X, Yamada E, Martin JN, et al. (2007) Innate partnership of HLA-B and KIR3DL1 subtypes against HIV-1. Nat Genet 39: 733–740.

Immunogenetics (2012) 64:669–678
DOI 10.1007/s00251-012-0628-y

ORIGINAL PAPER

Lineage-specific evolution of T-cell immunoglobulin and mucin domain 1 gene in the primates

Hitoshi Ohtani · Taeko K. Naruse · Yuki Iwasaki · Hirofumi Akari · Takafumi Ishida · Tetsuro Matano · Akinori Kimura

Received: 30 December 2011 / Accepted: 6 June 2012 / Published online: 19 June 2012

Abstract T-cell immunoglobulin domain and mucin domain containing protein 1 (TIM1), also known as a cellular receptor for hepatitis A virus (HAVCR1) or a molecule induced by ischemic injury in the kidney (KIM1), is involved in the regulation of immune responses. We investigated a natural selection history of *TIM1* by comparative sequencing analysis in 24 different primates. It was found that *TIM1* had become a pseudogene in multiple lineages of the New World monkey. We also investigated T cell lines originated from four different New World monkey species and confirmed that *TIM1* was not expressed at the mRNA level. On the other hand, there were ten amino acid sites in the Ig domain of TIM1 in the other primates, which were suggested to be under positive natural selection. In addition, mucin domain of TIM1 was highly polymorphic in the Old World monkeys, which might be under balanced selection. These data suggested that *TIM1* underwent a lineage-specific evolutionary pathway in the primates.

Keywords Natural selection · Molecular evolution · Pseudogene · TIM1 · Primate

Electronic supplementary material The online version of this article (doi:10.1007/s00251-012-0628-y) contains supplementary material, which is available to authorized users.

H. Ohtani · T. K. Naruse · A. Kimura (✉)
Department of Molecular Pathogenesis, Medical Research Institute, Tokyo Medical and Dental University,
1-5-45 Yushima, Bunkyo-ku,
Tokyo 113-8510, Japan
e-mail: akitis@mri.tmd.ac.jp

Y. Iwasaki · H. Akari
Center for Human Evolution Modeling Research, Primate Research Institute, Kyoto University,
Inuyama, Japan

T. Ishida
Unit of Human Biology and Genetics, Graduate School of Science,
The University of Tokyo,
Tokyo, Japan

T. Matano
AIDS Research Center, National Institute of Infectious Diseases,
Tokyo, Japan

Introduction

Comparative genomics is a useful tool for understanding the gene function from the view point of evolution. It has recently been reported that genes involved in regulation of immune system may have undergone the control of positive selection (Gibbs et al. 2007; Kosiol et al. 2008). The accelerated evolution may be due to a direct consequence of complex selection pressure exerted by infectious reagents including microbes and viruses (Barreiro and Quintana-Murci 2010). The known cases include genes of defensin family, which play crucial roles in antibacterial activity (Hollox and Armour 2008), and genes of APOBEC family, which are known to function as specific inhibitors against the infection of human immunodeficiency virus-1 (HIV-1) (Sawyer et al. 2004).

We previously performed a comparative genome analysis of primates and reported that genes encoding the immunoglobulin superfamily (IgSF) were classified into 11 functional categories based on the Gene Ontology (GO) database. The IgSF genes in three functional categories, immune system process (GO:0002376), defense response (GO:0006952), and multi-organism process (GO:0051704), had more chance to be under the positive natural selection than the IgSF genes in the other categories (Ohtani et al. 2011). In our previous comparative genome analysis, we focused on the orthologous

IgSF genes that appeared to be functional in all of human, chimpanzee, orangutan, rhesus macaque, and common marmoset. In other words, we excluded several genes of which an ortholog was considered to be non-functional, i.e., deleted gene, grossly rearranged gene, or pseudogene, in any of the five primate species. Such a lineage-specific destruction of IgSF genes, especially those involved in the immune response, may be interesting in view of the natural selection occurred during the evolution of primates. One of the excluded genes in our previous analysis was a gene for T-cell Ig domain and mucin domain containing protein 1 (TIM1), which was suggested to be a pseudogene due to an insertion in the common marmoset, while it should be functional in the other primates. TIM1 tightly linked to immune system, playing an important role in generation and/or maintenance of the balance between T helper 1 (Th1) cells and T helper 2 (Th2) cells, and it is up-regulated in Th2 cells after activation and interacts with its ligand expressed on antigen-presenting cells (de Souza and Kane 2006). *TIM1* can be found in the non-primate mammals including mouse and rat. However, *TIM1* orthologs are not found in the non-mammalian vertebrates such as chiken and zebrafish, implying that it might be involved in the mammalian-specific function. In addition, it was reported that *TIM1* is highly polymorphic in humans, but quite less polymorphic in chimpanzees, especially around the mucin domain (Nakajima et al. 2005). These observations suggested a unique evolutionary feature of *TIM1* in the primates.

In human, *TIM1* located on chromosome 5 at band q33 contains two distinct domains (Ig domain and mucin domain) (Khademi et al. 2004). It is known that TIM1 is a cellular receptor for hepatitis A virus (HAVCR1) in human (Feigelstock et al. 1998). TIM1 is also known to be induced in the kidney by ischemic injury and is called as kidney injury molecule 1 (KIM1) (Ichimura et al. 1998). It has been reported that *TIM1* polymorphisms are associated with various immune-related diseases and infectious diseases, including asthma, allergic rhinitis, atopic dermatitis, multiple sclerosis, type 1 diabetes, rheumatoid arthritis, AIDS, and cerebral malaria (Khademi et al. 2004; Kuchroo et al. 2003; McIntire et al. 2004; Meyers et al. 2005b; Su et al. 2008; Wichukchinda et al. 2010). These data implied that variations in *TIM1* might have been more or less selected during the evolution of humans.

In the present study, we determined nucleotide sequences of exons or equivalent regions of *TIM1* from 24 different primate species, including eight hominoids, six Old World monkeys, nine New World monkeys, and one prosimian, to investigate an evolutionary history of *TIM1*.

Materials and methods

Subjects

DNA samples from 24 primate species including human (*Homo sapiens*), chimpanzee (*Pan troglodytes*), bonobo (*Pan paniscus*), western gorilla (*Gorilla gorilla*), Bornean orangutan (*Pongo pygmaeus*), western black-crested gibbon (*Nomascus concolor*), lar gibbon (*Hylobates lar*), siamang (*Symphalangus syndactylus*), rhesus macaque (*Macaca mulatta*), long-tailed macaque (*Macaca fascicularis*), Hamadryas baboon (*Papio hamadryas*), mantled Guereza colobus (*Colobus guereza*), dusky leaf monkey (*Trachypithecus obscurus*), silver leaf monkey (*Trachypithecus cristatus*), Geoffroy's spider monkey (*Ateles geoffroyi*), white-fronted spider monkey (*Ateles belzebuth*), tufted capuchin (*Cebus apella*), common squirrel monkey (*Saimiri sciureus*), white-lipped tamarin (*Saguinus labiatus*), golden-handed tamarin (*Saguinus midas*), cotton-top tamarin (*Saguinus oedipus*), golden lion tamarin (*Leonthopithecus rosalia),* common marmoset (*Callithrix jacchus*), and Sunda slow loris (*Nycticebus coucang*) were the subjects.

Polymerase chain reaction (PCR) and sequencing analysis

Sequence information for homologous regions to the coding regions of human *TIM1* was obtained from 24 primate species by direct sequencing of PCR products from the genomic DNA samples. Primers used for PCR and direct sequencing were designed by referring the human, chimpanzee, rhesus macaque, common marmoset gene sequences, and whole-genome shotgun sequences from prosimians deposited in the UCSC Genome Browser and NCBI BLAST (http://blast.ncbi.nlm.nih.gov/Blast.cgi) (Supplemental Table S1). PCR condition was composed of a denaturing step (94 °C for 2 min), 35 cycles of chain reaction (94 °C for 30 s, 56 °C for 30 s, and 72 °C for 1 min), and a final extention step (72 °C for 5 min). The PCR products were then purified and sequenced by the BigDye Terminator cycling system using an ABI3130x automated DNA sequencer (Applied Biosystems, Foster City, CA, USA). Editing and assembly of sequences were done by using SEQUENCHER (Gene Codes, Ann Arbor, MI, USA). When sequence variations (heterozygous sequences) in a specific species were detected, the sequences which were more conserved among 24 primate species were considered as ancestral sequences and used for statistical analyses. The *TIM1* sequences determined in this study were deposited in DNA Data Bank of Japan (DDBJ) (Supplemental Table S2).

Expression analysis of *TIM1*

Total RNA was extracted from a human T cell line, Jurkat, and four different T cell lines originated from the New World monkeys, HSF-10 (tufted capuchin), HSQ-115 (common squirrel monkey), HST-3 (white-lipped tamarin) (Akari et al., manuscript in preparation), and HSCj-109 (common marmoset) (Hohjoh et al. 2009), by using RNAiso (TaKaRa Bio Inc., Shiga, Japan). Extracted RNAs (500 ng) were subjected to reverse transcription (RT) by using RT reagent Kit (TaKaRa Bio Inc., Shiga, Japan). Aliquots of RT products were used for the expression analysis of *TIM1*. Primers for PCR were designed in the highly conserved regions of *TIM1* among human and the New World monkeys (Supplemental Table S3). PCR condition was the same as that described in the previous section.

Diversity of TIM1 mucin domain in the Old World monkeys

Nucleotide sequences for the mucin domain from eight samples of rhesus macaques were determined by sequencing of PCR products, which were cloned into pT7Blue Blunt vector and transformed Nova Blue Single Competent cells using the Perfectly Blunt cloning kit (Novagen Inc., Madison, WI). Colony PCR was used to identify positive clones, and at least 20 positive clones from each sample were subsequently sequenced as described previously. We also examined length variations of exon 4 from 16 rhesus macaques and 10 crab-eating macaques by direct sequencing of the PCR products.

Statistical analyses

We used both Bn-Bs program and PAML program as described previously (Ohtani et al. 2011). In brief, the Bn-Bs program was used to investigate the presence of branch-specific positive selection (the branch model). The Bn-Bs program estimates the values of non-synonymous substitution rate (dn) and synonymous substitution rate (ds) based on the modified Nei–Gojobori method, where a phylogenetic tree is given (Zhang et al. 1998). The value of ω, an abbreviation for the value of dn/ds, is a criterion of natural selective pressure acting on the gene, and the modified Nei–Gojobori method has been used for estimating non-synonymous/synonymous substitution rates (Nei and Gojobori 1986). Statistical significance of the difference between dn and ds was examined by *Z*-test (Chatterjee et al. 2009). An ordinary least-squares method was used to estimate branch lengths and variances for *Z*-test. The least-squares method gives estimates for evolutionary distances among the analyzed sequences (Rzhetsky and Nei 1993). The PAML program version 4.7 was used to investigate the presence of site-specific positive selection (the site model). The site model treats ω allowing the variance among codons (Yang 2005; Yang and Nielsen 2000), and the following null and alternative models were implemented in the site model: M0 (null), M1a (nearly neutral), M2a (positive selection) (Wong et al. 2004), M3 (discrete), M7 (beta), and M8 (beta and ω) (Yang and Nielsen 2000). The likelihood ratio tests (LRT) of three pairwise comparisons, i.e., comparisons of M1a vs. M2a, M1a vs. M3, and M7 vs. M8, determined whether particular models would provide a significantly better fit. When the LRT suggested positive selection, the Bayes empirical Bayes (BEB) method was used to detect the sites under the positive selection (Yang et al. 2005). To investigate a possible selection operated on exon 4 region of *TIM1* alleles in rhesus macaques, we calculated Tajima's *D* (Tajima 1989; Tamura et al. 2011).

Results

TIM1 is non-functional in several lineages of New World monkey

TIM1 is a member of *TIM* gene family composing of *TIM1*, *TIM3*, and *TIM4*, in the human genome (Khademi et al. 2004). In the previous comparative genome analysis, we searched for orthologous genes for human *TIM1*, *TIM3*, and *TIM4* in the genome of chimpanzee, orangutan, rhesus macaque, and common marmoset by using the UCSC/MULTIZ alignment program. It was found that there was an insertion of 205 bp in exon 2-equivalent region in the common marmoset gene, which would generate multiple frameshift/nonsense mutations in the coding sequence and/or destroy the splicing junction.

To confirm the presence of deleterious insertion in *TIM1* in the genome of common marmoset and possibly in other primate genomes, we determined nucleotide sequences for exons or equivalent regions of *TIM1* from 24 primate species including human, chimpanzee, orangutan, rhesus macaque, and common marmoset. For this purpose, we designed primers by referring the known *TIM1* sequences (Supplemental Table 1). The sequencing analysis of the genomic gene for *TIM1* revealed the deleterious insertions of 206–212 bp in several New World monkeys, i.e., golden lion tamarin (212 bp), cotton-top tamarin (206 bp), white-lipped tamarin (207 bp), and golden-handed tamarin (210 bp) (Supplemental Figure S1). It was speculated that the insertion had been occurred within a sequence stretch of 13 bp, AGCCTCATCCTAC, corresponding to codons 9–13, because these sequences were repeated and flanked the insertion in the genomes of common marmoset and cotton-top tamarin, and there were a few substitutions in this sequence stretch from the other New World monkeys (Supplemental Figure S1). The inserted sequences belong to the

LINE/L1 (L1PA7) repeat, which contain a poly A stretch at one end in a reverse orientation to the TIM1 coding sequences, and homologous sequences can be found as multiple copies in the marmoset genome. On the other hand, we found nucleotide substitutions in exon 3-equivalent regions, which resulted in termination mutations in three other New World monkeys not carrying the insertion, common squirrel monkey (S84X), tufted capuchin (V22X), and Geoffroy's spider monkey (C36X) (Fig. 1). Among the New World monkey species investigated in this study, only the white-fronted spider monkey appeared to carry a functional gene for TIM1.

To investigate whether *TIM1* was non-functional in the New World monkey lineages, we performed RT-PCR analysis of mRNA expression in T cell lines originated from human, tufted capuchin, squirrel monkey, white-lipped tamarin, and common marmoset. As illustrated in Fig. 2a, two pairs of primers were used in the RT-PCR analysis, where forward primers were designed in exon 3 and junction of exon 5–exon 6, while reverse primers were designed in exon 9 and junction of exon 5–exon 6 (Supplemental Table S3). The *TIM1* expression was confirmed in the human T cell line, but could not be detected in the T cell lines from the New World monkeys carrying either the insertions (common marmoset and white-lipped tamarin) or the nonsense mutations (common squirrel monkey and tufted capuchin) (Fig. 2). No expression of *TIM3* and *TIM4* was observed in the T cell lines from human and the New World monkeys (data not shown).

Positive selection sites of *TIM1* in the primates

In the other primate species than the New World monkey, *TIM1* appeared to be functional, and there were many substitutions. When we calculated the dn and ds values in each primate lineage, it was found that the dn values were higher

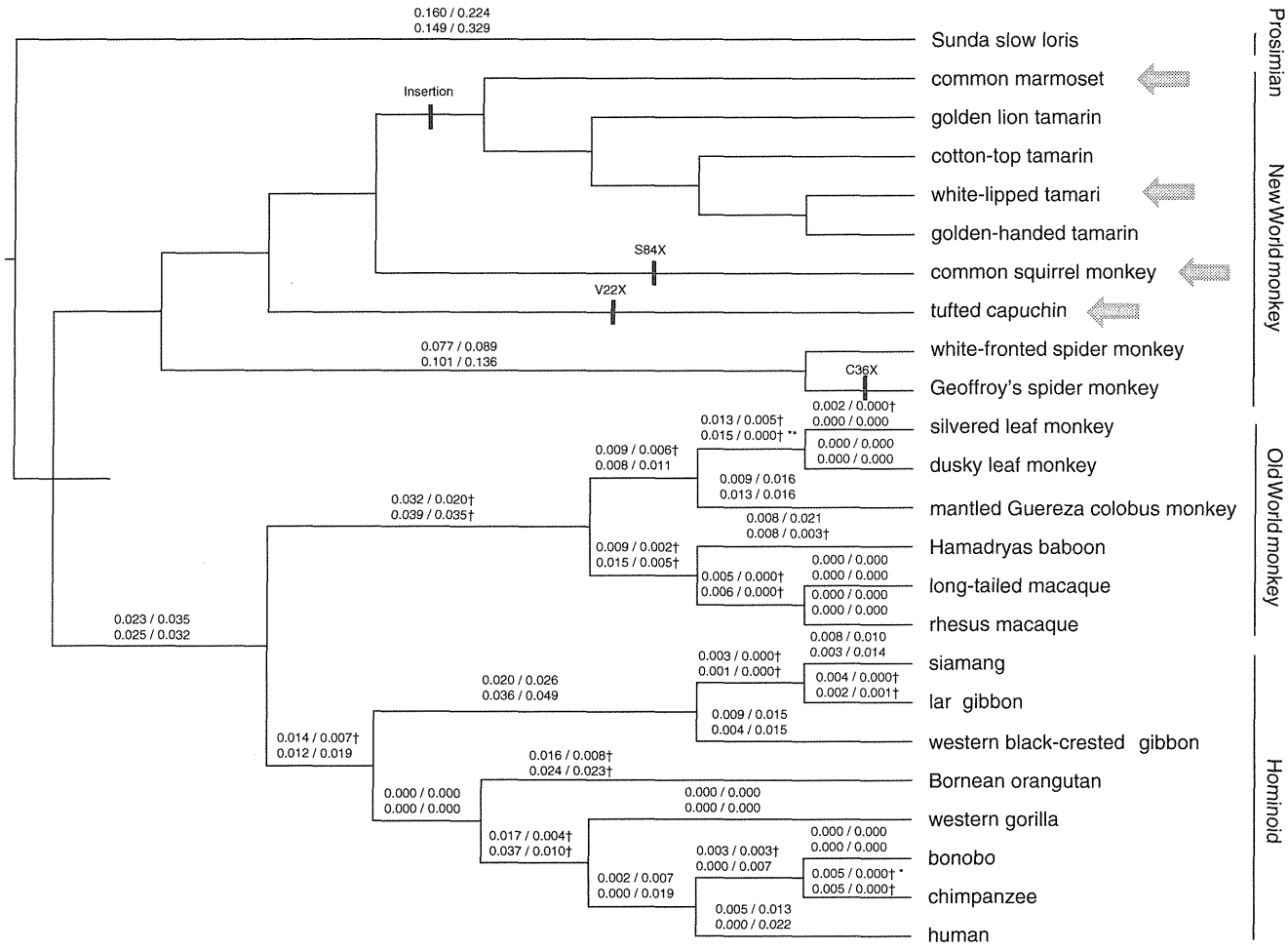

Fig. 1 Phylogenetic trees for TIM1 in the primate evolution. Values above branches indicate estimated values of dn and ds per lineage by using the Bn-Bs program. Upper values are for the entire coding region, while lower values are for the Ig domain. *Daggers* indicate that the dn value was higher than the ds value. *Asterisks* indicate that there is a significant difference between the dn and ds values ($^{**}p<0.01$; $^{*}p<0.05$; *Z*-test). *Vertical lines* indicate that *TIM1* had become pseudogene in the specific lineage. *Arrows* indicate the species for which the mRNA expression of *TIM1* in T cell line was investigated

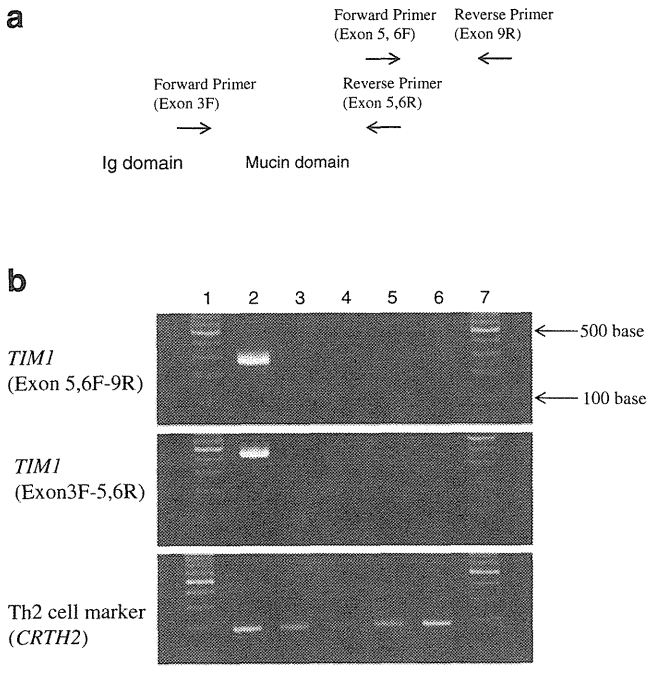

Fig. 2 Expression of *TIM1* in T cell lines. **a** TIM1 cDNA is schematically shown. *Arrows* indicate the regions of PCR primers which were designed in the highly conserved coding regions of *TIM1* among human and New World monkeys. **b** From *left* to *right*: *lane 1* 100-bp ladder size marker, *lane 2* Jurkat (human), *lane 3* HSF-10 (tufted capuchin), *lane 4* HSQ-115 (common squirrel monkey), *lane 5* HST-3 (white-lipped tamarin), *lane 6* HSCj-109 (common marmoset), and *lane 7* 100-bp ladder size marker. A marker gene (*CRTH2*) was used as a positive control of gene expression because it is known to be expressed in T cells especially in Th2-type cells

than the ds values in several lineages, especially in the Old World monkeys (Fig. 1). Sequence alignment of TIM1 at the amino acid (AA) level in the primates is shown in Fig. 3. To identify possible target sites for positive selection, we analyzed the TIM1 sequences by the BEB method. Sixteen TIM1 sequences from primate species, human, chimpanzee, bonobo, western gorilla, Bornean orangutan, western black-crested gibbon, lar gibbon, siamang, rhesus macaque, long-tailed macaque, Hamadryas baboon, mantled Guereza colobus, dusky leaf monkey, silver leaf monkey, white-fronted spider monkey, and Sunda slow loris, were used in the statistical test. It was revealed that 14 AA sites, at 23, 25, 30, 37, 51, 54, 58, 59, 72, 93, 102,120, 125, and 288 positions equivalent to the human TIM1, were the positively selected sites. These 14 AA sites were highly variable among the 16 primate sequences, e.g., AA site at 23 was lysine in hominoid; asparagine in rhesus macaque, long-tailed macaque, Hamadryas baboon, and mantled Guereza colobus; tyrosine in dusky leaf monkey and silver leaf monkey; serine in white-fronted spider monkey; and glutamine in Sunda slow loris. Most of the positive selection sites (10/14: 71.4 %) were found in the Ig domain (Fig. 3a, b).

Diversity of TIM1 in the Old World monkey

As shown in Fig. 3, a large number of deletion/insertion events were observed in the mucin domain (Fig. 3b, c). It was reported that human TIM1 exhibited a high degree of amino-acid variability in the mucin domain (Nakajima et al. 2005). Because the mucin domain of TIM1 encoded by exon 4 might be under the positive selection in the Old World monkey (Supplemental Table S4), we investigated the diversity of TIM1 in rhesus macaques by determining nucleotide sequences for the mucin domain from eight samples (16 haplotypes). As shown in Fig. 4, a high level of sequence diversity with multiple insertion/deletion of 18-bp sequences, A(T/C)GACAAC(G/A)(A/G)C(T/C)CT(T/G)CCA forming a part of AA stretch Thr-Thr-Thr-Thr-Leu-Pro (TTTTLP), was observed in the mucin domain of rhesus TIM1. We then investigated a possible selection by using the Bn-Bs program, but no statistically significant data were obtained, presumably because the compared sequences were not long enough to give a definite conclusion. However, when we calculated Tajima's *D* for these *TIM1* alleles, a value of 0.607 was obtained, which suggested a balanced selection of polymorphisms in the mucin domain of TIM1 in the Old World monkey.

On the other hand, because the diversity of mucin domain in the rhesus macaques could be detectable as a length diversity of exon 4, we examined length variations of *TIM1* exon 4 in additional samples of rhesus and long-tailed macaques. It was found that the length polymorphism was due to the repeat number polymorphisms or insertion/deletion polymorphisms of 18-bp unit and its components of 3- and 6-bp repeats (Supplemental Table S5).

Discussion

In this study, we investigated sequence diversity in the protein coding exons of *TIM1* from various species by direct sequencing method. Although there were a few sites with heterozygous sequences, we used "evolutionary conserved" sequences obtained from each sample in the statistical analyses so that the substitutions were underestimated in this study. Even though there was an underestimation, we demonstrated that the Ig domain of TIM1 has been under the positive selection during the course of primate evolution. Another interesting finding was that TIM1 has undergone pseudogene evolution in the New World monkey. It was suggested that the generation of pseudogene had occurred several times over the New World monkey lineages, by the insertion of deleterious sequences or base substitutions leading to a termination codon. Similar natural selection pattern was reported for type 1 vomeronasal receptors (*V1RL*), in which the pseudogene generation had independently

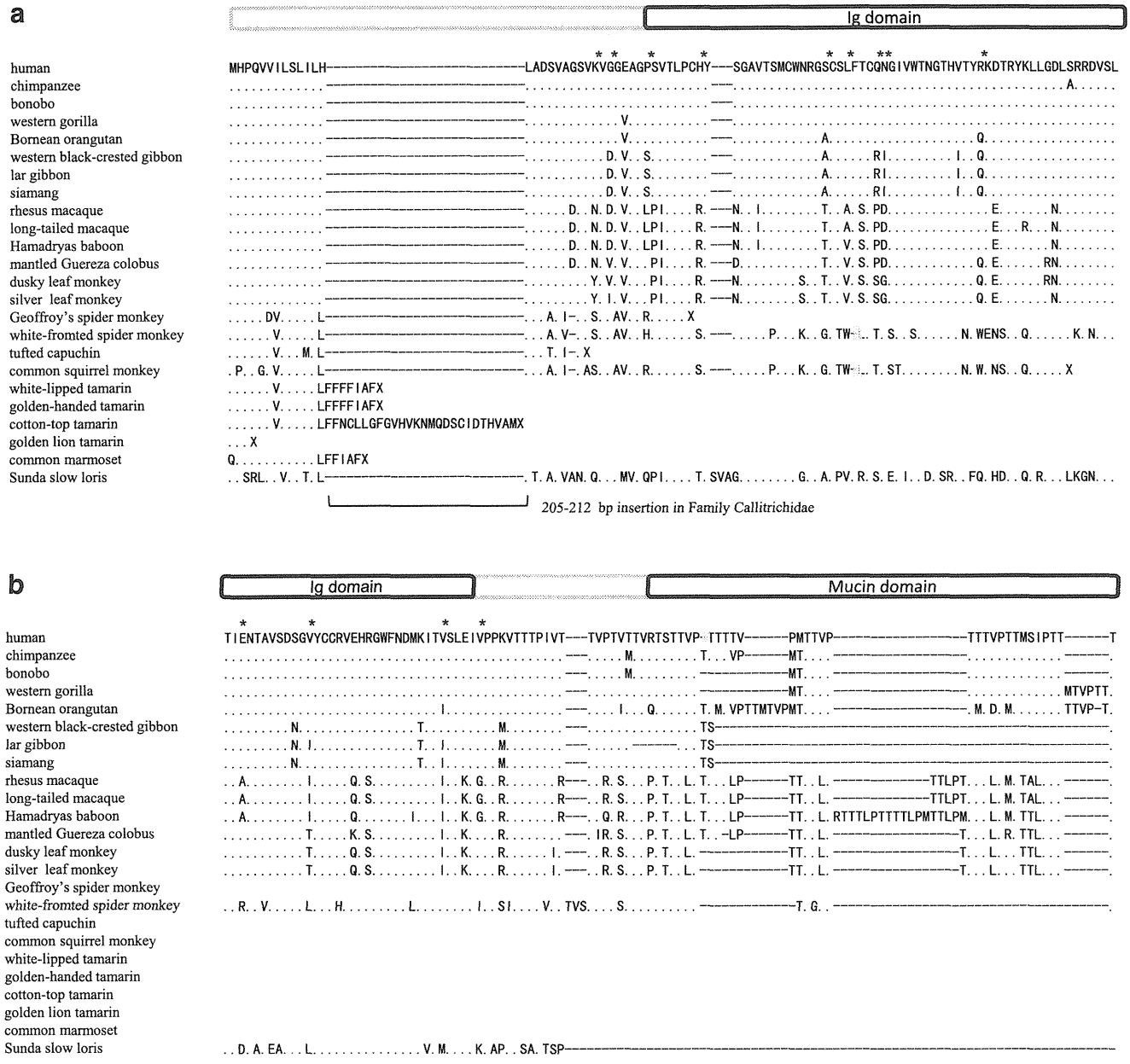

Fig. 3 Alignments of TIM1 amino acid sequences from 24 primate species. *Dots* indicate identities to the human reference sequence, while *dashes* indicate alignment gaps. *Asterisks* indicate AA sites identified as being under the significant positive selection ($p<0.05$). **a**, **b**, **c**, and **d** represent quarter parts of TIM1 from N-terminus to C-terminus. Ig and mucin domains are schematically indicated

occurred in the human and other primate lineages, implying that the function of *VIRL* might be highly lineage specific (Mundy and Cook 2003).

TIM1 plays an important role in generation and/or maintenance of the balance between Th1 and Th2 cells (Su et al. 2008). It is known that a natural ligand for TIM1 is T-cell Ig domain and mucin domain containing protein 4 (TIM4) (Meyers et al. 2005a), and the interaction of TIM1 with TIM4 plays a crucial role in sustaining the polarization status of Th2 cells (Khademi et al. 2004; Mariat et al. 2005). Because TIM1 expressed on the surface of Th2 cells regulated the immune response by modulating cytokine production in mammals, the Th1/Th2 balance might be skewed or affected by the lack of TIM1 in the most lineages of New World monkey. Previous study demonstrated that expression of Th1-type cytokines, IFN-γ and TNF-β, was considerably lower than that of Th2-type cytokines, IL-4 and IL-10, in a New World monkey, owl monkey (Pico de Coana et al. 2004). This observation may support the disturbance of Th1/Th2 balance in the owl monkey lacking TIM1, although we cannot exclude a possibility that some other molecules than TIM1 might regulate Th1/Th2 balance

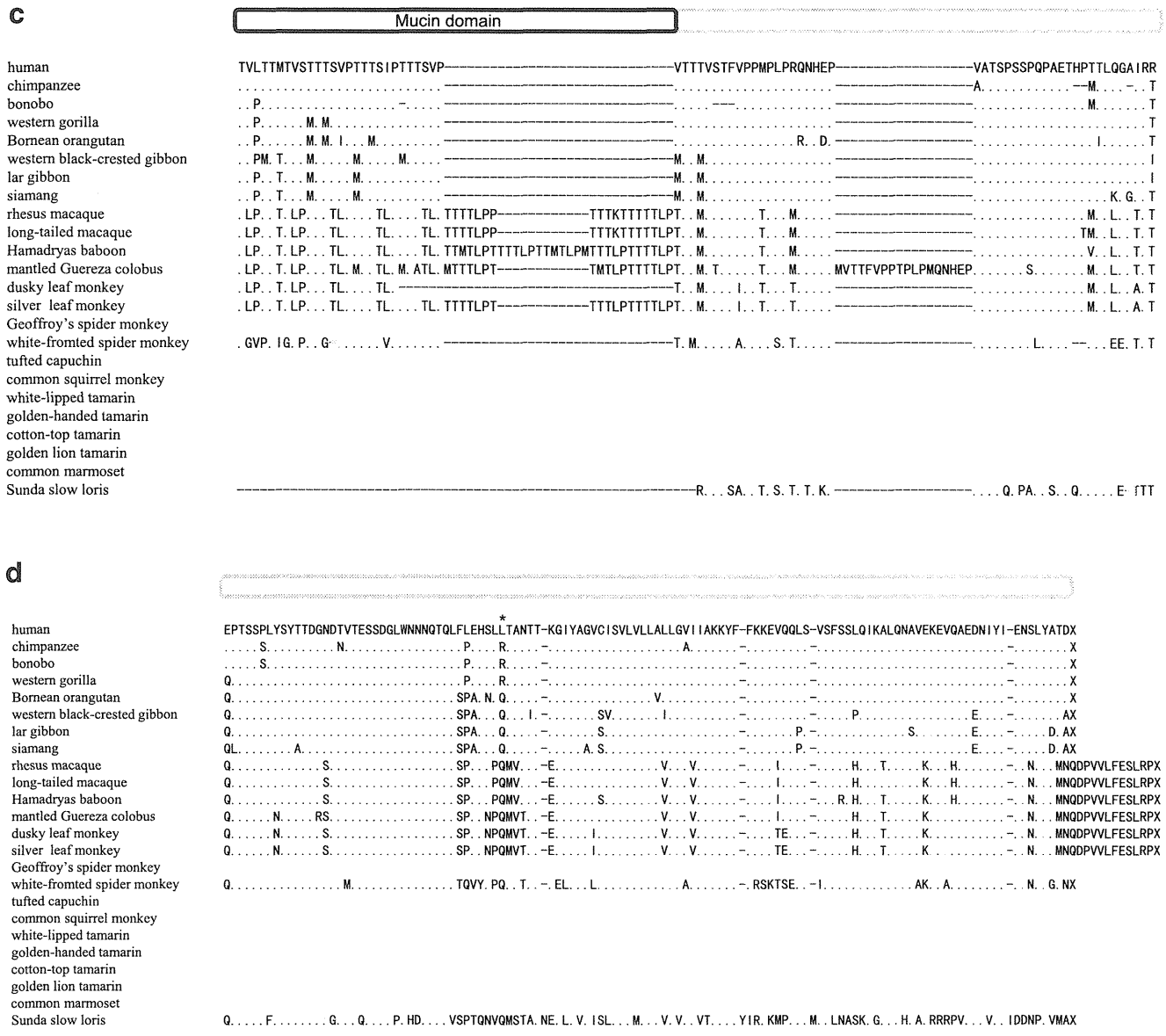

Fig. 3 (continued)

in the primates including the TIM1-deficient New World monkey. It is interesting to note that there is a *TIM1*-like gene on chromosome 13 in the marmoset genome, which might replace the function of *TIM1*. However, this TIM1-like gene lacks introns and contains several in-frame stop codons, when it is aligned with human *TIM1* (Supplemental Figure S2).

It is known that TIM1 is a cellular receptor for hepatitis A virus (HAV) in human (Feigelstock et al. 1998). The results in this study suggested that the New World monkey lineages

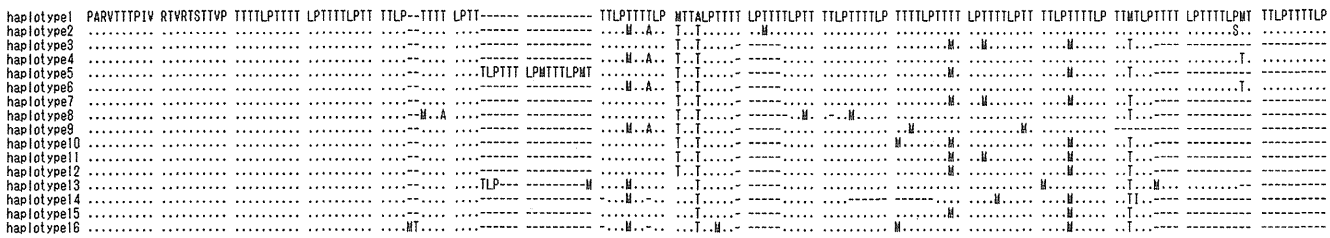

Fig. 4 Diversity of the mucin domain in rhesus macaques. *Dots* indicate identities to the haplotype 1 sequence, while *dashes* indicate alignment gaps

might lack a cellular receptor for HAV, TIM1. However, because the New World monkey is susceptible to HAV infection (Mathiesen et al. 1980), further studies are needed to clarify or find other cellular receptors for HAV in the New World monkey and a cause or reason of pseudogene generation, which had occurred in several lineages of the New World monkey. In addition, it has been reported that TIM1 polymorphisms are associated with resistance to autoimmune diseases including multiple sclerosis, which are associated with the imbalance between Th1 and Th2 cells (Khademi et al. 2004). Nevertheless, common marmosets are used as an animal model for multiple sclerosis, experimental autoimmune encephalomyelitis (Uccelli et al. 2003). Thus, susceptibilities of the New World monkey to the autoimmune diseases should be investigated in relation to the non-functional TIM1.

In this study, 14 AA sites of TIM1 were identified as positively selected sites in the evolutional course of primates other than the New World monkey. It was suggested that the Ig domain of TIM1 was a binding site for HAV (Feigelstock et al. 1998). In addition, structural conformation of the mucin domain is required for the efficient viral entry (McIntire et al. 2003). In this study, TIM1 was considered to be under the significant positive natural selection in the Ig domain, prompting us to investigate the three dimensional (3D) structures of the Ig domains using SWISS-MODEL, an Automated Comparative Protein Modeling Server (http://swissmodel.expasy.org/SWISS-MODEL.html) (Bordoli et al. 2009). As shown in Fig. 5, it was suggested that most of the target sites for the positive selection accumulated on the surface of Ig domain. These observations support a hypothesis that the evolution of TIM1 in the primates might be driven by exogenous pathogens. The positively selected sites in the Ig domain of TIM1 in the primates other than the New World monkey and a high level diversity in the mucin domain of TIM1 in the Old World monkey might be a direct consequence of a selection pressure exerted by HAV. However, because TIM1 polymorphisms are also associated with other infectious diseases including HIV/AIDS and cerebral malaria, further functional studies are required to clarify the mechanism of natural selection at specific sites of Ig and mucin domains of TIM1. For example, we are now investigating whether the TIM1 repeat polymorphism would influence the production level of neutralizing antibodies against challenging Simian Immunodeficiency Virus (SIV) in experimental models of SIV vaccination in rhesus macaques (Sugimoto et al. 2010; Ishii et al. 2012; Nomura et al. 2012).

Because TIM1 is known to interact with TIM4 and both Ig and mucin domains of TIM1 are involved in this interaction (Meyers et al. 2005a), one might speculate a co-evolution of TIM1 and TIM4. It should be noted here that human TIM family includes three members, TIM1, TIM3, and TIM4, while mouse TIM family includes eight members, TIM1 toTIM8. Although we searched for orthologs of mouse TIM2, TIM5, TIM6, TIM7, and TIM8 in the common marmoset genome by using Blat program (http://genome.ucsc.edu/cgi-bin/hgBlat), we could not detect any orthologous genes. Therefore, TIM family in the New World monkey consists of only two functional members, TIM3 and TIM4. Then, we investigated a possible evolutionary selection of TIM3 and TIM4. However, no significant positive selection appeared to operate on the evolution of TIM3 and TIM4 in the primates (Supplemental Table S6). A marginal and non-significant positive selection for TIM4 in chimpanzee was observed, but it may not correlate with co-evolution of TIM1 and TIM4, because the mucin domain of TIM1 is virtually non-polymorphic in chimpanzee (Nakajima et al. 2005). Nevertheless, the observations in this study suggest that the diversity of TIM family is widely ranged among mammalian species. It may be of interest to investigate whether the binding affinity of TIM1 and TIM4 would be affected by the TIM1 variations in future experiments. On the other hand, it may be noteworthy that TIM1, TIM3, and TIM4 can independently serve as receptors for phosphatidylserine to mediate uptake of apoptotic cells (Kobayashi et al. 2007; Freeman et al. 2010), implying that their cooperation would be dispensable in some functional aspects.

In conclusion, we investigated the molecular evolution of TIM1 in 24 primate species. TIM1 had become pseudogenes in most lineages of the New World monkey, while it

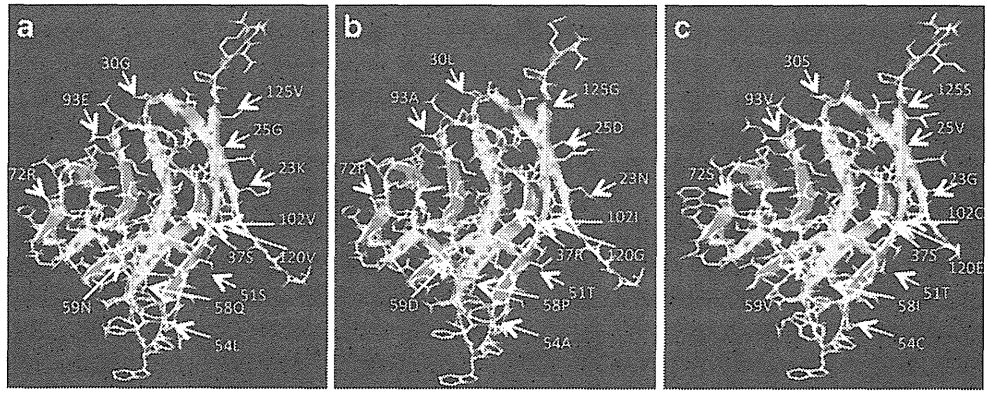

Fig. 5 Three-dimensional structures of TIM1 modeled by SWISS-MODEL. *Arrows* indicate AA sites identified as being under the positive selection by using the BEB method in the PAML program. **a** human TIM1, **b** rhesus macaque TIM1, **c** long-haired spider monkey TIM1